MPMI Vol. 38, No. 5, 2025, pp. 762–777, https://doi.org/10.1094/MPMI-11-24-0149-R

RESEARCH

Cellular Responses in the Pigeonpea Wild Relative *Cajanus platycarpus* to *Helicoverpa armigera* Herbivory: The Role of Methionine Sulfoxide Reductase B1 (*CpMSRB1*) in Enhanced Defense

Maniraj Rathinam,[1] Narasimham Dokka,[1] Kameshwaran Senthil,[1] Shivangi Mahawar,[2] Shaily Tyagi,[1] Dineshkumar Rengarajan,[3] Preethi Vijayaraghavareddy,[4] Yuvaraj Iyyappan,[1] Basavaraj Y. B.,[5] Sandeep Reddy,[4] Vinutha T.,[3] Rama Prashat G.,[6] Subodh Kumar Sinha,[1] Prasanta K. Dash,[1] Sheshshayee Sreeman,[4] Manoj Majee,[2] and Rohini Sreevathsa[1,†]

[1] ICAR-National Institute for Plant Biotechnology, New Delhi, India
[2] National Institute of Plant Genome Research, New Delhi, India
[3] Division of Biochemistry, ICAR-Indian Agricultural Research Institute, New Delhi, India
[4] Department of Crop Physiology, University of Agricultural Sciences, GKVK, Bangalore, India
[5] ICAR-Indian Agricultural Research Institute, Regional Station, Aundh, Pune, Maharashtra, India
[6] Division of Genetics, ICAR-Indian Agricultural Research Institute, New Delhi, India

Accepted for publication 28 April 2025.

Understanding key cellular mechanisms leading to improved defense against various stressors is essential for cultivating robust nutritious crops capable of flourishing in diverse environments. We present an in-depth characterization of the defense response in the pigeonpea wild relative *Cajanus platycarpus* to herbivory by pod borer *Helicoverpa armigera.* To fight the attacking pest, *C. platycarpus* strategically activated non-enzymatic reactive oxygen species (ROS) scavengers and unleashed methionine sulfoxide reductases to safeguard the integrity of methionine residues. We unveiled for the first time physical interaction between *Cp*MSRB1 and chorismate mutase (*Cp*CM1.1), a pivotal player in the phenylpropanoid pathway. This association fueled the synthesis of phenylpropanoids and enhanced ROS scavenging crucial for repelling herbivores. Repairing *Cp*CM1.1 also boosted salicylic acid production, coordinating defense signaling with jasmonic acid. Additionally, heterologous expression of *CpMSRB1* in tomato improved defense against herbivory by enhanced ROS scavenging and polyphenol production. This study demonstrates the role of *Cp*MSRB1 in protecting a major enzyme in the shikimate pathway, reinforcing defense against *H. armigera*.

Keywords: herbivory, methionine sulfoxide reductase, phenylpropanoids, reactive oxygen species, wild relative

Exploring plant defense mechanisms during interactions with stress factors is crucial for improving crop resilience amid the changing climate and growing population. Gaining insights into plant responses to environmental challenges enables the development of crops that withstand adversity while maintaining productivity. This understanding is essential for advancing food security and sustainable agriculture in the face of global climate shifts (Rathinam et al. 2022). Reactive oxygen species (ROS) are naturally produced in plants as a result of cellular activities (Tyagi et al. 2022b). Though they are essential during stress signaling, plant growth, and developmental processes, maintaining a careful ROS balance is critical for cellular function. Redox homeostasis thus refers to the balance between oxidative stress and cellular antioxidant defense system within a cell (Ali et al. 2023). On the other hand, sustained stress can increase ROS levels, causing damage to macromolecules and eventually leading to cell death. Like many other stress factors, sustained herbivory also triggers a surge in ROS levels (Bittner et al. 2017; Goggin and Fischer 2022). The initiation of insect feeding triggers a wide range of plant defense responses, including the induction of ROS production to counter the attack (Bittner et al. 2017; Goggin and Fischer 2022). In this situation, the ability of plants to resist or succumb to insect attacks depends on precisely regulating ROS levels, ensuring the continuous expression of essential proteins.

†Corresponding author: R. Sreevathsa; rohinisreevathsa@gmail.com and Rohini.Sreevathsa@icar.gov.in

Author contributions: R.S. and M.R. conceived the study. M.R., N.D., K.S., S.M., Y.I., and R.S. developed the methodology. M.R., N.D., K.S., S.M., S.T., D.R., P.V., S.R., and R.P.G. conducted the formal analysis. M.R., N.D., K.S., S.M., Y.I., and R.S. conducted the investigation. R.S., V.T., S.K.S., P.K.D., B.Y.B., S.S., and M.M. provided the resources. M.R., N.D., K.S., S.M., S.T., P.V., and Y.I. curated the data. M.R., N.D., and Y.I. wrote the original draft. R.S. reviewed and edited the manuscript. M.R. and N.D. performed the visualization. R.S. supervised the study and acquired the funding.

Data availability: Data are available from the authors and will be provided upon reasonable request.

Funding: This work was supported by the Science and Engineering Research Board, New Delhi, India (grant number CRG/2019/001261). Support for the publication costs for this article was provided in part by Microbes Biosciences.

e-Xtra: Supplementary material is available online.

The author(s) declare no conflict of interest.

As an adaptive strategy, plants have evolved a diverse array of ROS scavengers to manage their dual-edged effects. These include enzymatic and non-enzymatic scavengers, as well as enzymes dedicated to repairing oxidative damage. These mechanisms repair and prevent free radical damage to macromolecules (Ali et al. 2023; Rey and Tarrago 2018). To enhance cellular level tolerance and fortify stress management, plants strategically coordinate the simultaneous production of scavengers and repair enzymes with precision and efficiency.

In plant systems, an important process is the regulation of redox post-translational modifications, in which key methionine-rich proteins are oxidized during oxidative stress (Rathinam et al. 2022). As a sulfur-containing amino acid, both free-form and peptide-bound L-methionine are highly prone to oxidation by ROS (Jacques et al. 2015). Free methionine serves a vital role as an antioxidant, whereas methionine within peptides is essential for maintaining flexibility to support the activity of protein structures (Gustavsson et al. 1999). Disrupting the redox balance of cellular methionine impairs antioxidant proteins, leading to increased ROS production and accumulation. Therefore, to ensure uninterrupted cellular activities amidst prolonged stress, plants must prioritize redox homeostasis. One of the conventional mechanisms in the mitigation of redox post-translational modifications is the categorical involvement of methionine sulfoxide reductases (MSRs) (Martí-Guillén et al. 2022; Rathinam et al. 2022; Rey and Tarrago 2018). These are enzymes that are fundamental in preserving the cellular activity of antioxidant enzymes by reversing methionine oxidation in the peptide side chains. Under stress conditions, MSRs play a crucial role in safeguarding the redox status of cellular methionine, thereby maintaining redox homeostasis (Rey and Tarrago 2018).

MSRA and MSRB are two types of plant MSRs that reduce peptide-bound methionine, and the free form of methionine is also reduced by MSRA (Hazra et al. 2022; Rey and Tarrago 2018). Research findings have highlighted a spectrum of enzymes as MSR substrates that are involved in diverse pathways crucial for managing oxidative stress, such as catalase (Cui et al. 2022), peroxidase (Xiao et al. 2021), glutathione S-transferase (Zhao et al. 2022), heme oxygenase (Ding et al. 2021), and RUBISCO (Cui et al. 2022). The association of MSRs with oxidative stress management has also been well demonstrated in various model and crop plants under biotic and abiotic stress conditions (Cui et al. 2022; Ding et al. 2021; Hazra et al. 2022; Hu et al. 2023; Xiao et al. 2021; Zhao et al. 2022). Understanding the role of MSRs in insect herbivory and how plants manage ROS under sustained attack is crucial for developing effective pest management strategies in crops.

Previously, we demonstrated the pivotal involvement of MSRs in the resistance response of *Cajanus platycarpus*, a wild relative of pigeonpea, against herbivory inflicted by the notorious polyphagous pest *Helicoverpa armigera* (Rathinam et al. 2019, 2022). Furthermore, we uncovered an atypical strategy in *C. platycarpus* for handling ROS during herbivory. This involved simultaneous induction of polyphenols and downregulation of genes encoding antioxidant enzymes (Rathinam et al. 2022). The act of MSR-mediated redox homeostasis in the wild relative during herbivory was predominantly driven by two *MSR* genes, *CpMSRB1* and *CpMSRA2*, that co-expressed with genes involved in redox management and secondary metabolite production (Rathinam et al. 2022). This raised an intriguing question about the possible association of the two pathways during redox management in the wild relative, despite the downregulation of ROS scavengers. Furthermore, continued research in our lab on understanding the molecular mechanisms of resistance in the wild relative to *H. armigera* delved on an active reprogramming of the phenylpropanoid pathway (Rathinam et al. 2019, 2020; Tyagi et al. 2022a). In light of these discoveries, can there be a conceivable connection between MSR-mediated redox homeostasis and the orchestration of secondary metabolism? Should such a connection exist, the resulting insights could prove not only remarkable for deciphering the biology of the wild relative but also for diving deeper into the novelty of *CpMSRB1*. Thus, the goal of this study was to define the intricacies of the defense response in *C. platycarpus* when exposed to sustained herbivory. These findings may reveal connections between the regulation of secondary metabolism and redox homeostasis and thereby enable the development of holistic approaches to manage various stresses centered on ROS regulation.

Results

ROS homeostasis is essential for effective defense response in *C. platycarpus* under continued herbivory by *H. armigera*

As with other stress factors, regulating ROS surge during sustained herbivory is crucial for maintaining cellular functions and reinforcing defense mechanisms (Tyagi et al. 2022b). In our earlier studies on deciphering the resistance mechanism of the pigeonpea wild relative to herbivory by *H. armigera*, we observed the importance of ROS management as a crucial parameter for improved defense (Rathinam et al. 2022). In the present study, we therefore envisaged characterizing in depth redox management in the wild relative during *H. armigera* feeding.

The primary understanding of ROS homeostasis under herbivore challenge in *C. platycarpus* was gained by examining how superoxide and hydrogen peroxide (H_2O_2) radicals were managed. Both nitroblue tetrazolium (NBT) staining and spectrophotometric measurement of H_2O_2 in the challenged leaves revealed that the wild relative accumulated ROS by 24 h of herbivory that decreased by 48 and 96 h, suggesting increased early scavenging (Fig. 1A and B). Additional evidence on the pattern of ROS management was provided by the total polyphenol content, which showed alterations as insect feeding continued. Compared with 0 h (without herbivory), there was an abrupt increase in the total polyphenol content by 24 h of herbivory, which decreased thereafter (48 and 96 h; Fig. 1C). ROS scavenging capacity, as assessed by DPPH (2,2-diphenyl-1-picrylhydrazyl) activity, also showed increased scavenging after 24 h of herbivore challenge, which was maintained thereafter (Fig. 1D). This corroboratory evidence demonstrated hastened ROS scavenging and increase in total phenol content to be in tandem, suggesting a close relationship between them.

In our earlier study, we observed the downregulation of genes encoding ROS scavenging enzymes, in contrast to the total phenolic content (Rathinam et al. 2022). In this study, we assessed the activities of antioxidant enzymes such as superoxide dismutase (SOD), catalase (CAT) and glutathione reductase (GR). The analyses confirmed the absence of any significant variation in the activities of CAT and GR to herbivory (Fig. 1E and F), whereas SOD activity reduced at the 96-h time point (Fig. 1G). The fact that the activity of scavenging enzymes was unaltered further highlighted the possible role of non-enzymatic antioxidants in the management of ROS during continued herbivory in the wild relative.

CpMSRB1: A novel player in the resistance response of *C. platycarpus* to *H. armigera*

In our previous study on plant-herbivore interactions, we highlighted the significance of *MSR* genes and identified *CpMSRA2* and *CpMSRB1* as responsive to *H. armigera* infestation (Rathinam et al. 2022). *Cp*MSRB1 was found to be localized in the plastid and co-expressed with plastidial proteins involved in the defense response (Rathinam et al. 2022). Plastids are

intricately connected to defense response through the phenylpropanoid pathway due to both their role in the biosynthesis of precursor molecules and their involvement in stress responses that regulate phenylpropanoid production. This led us to further characterize the plastidial *Cp*MSRB1 to unravel its functional role in the wild relative-pod borer interaction.

To investigate this, we first analyzed the response of *CpMSRB1* to herbivore attack. Expression profiling across different time points showed a progressive increase in *CpMSRB1* transcript accumulation (Fig. 2A), increasing at 24 h and sustaining until 96 h of herbivory. This pattern suggested a functional role for *CpMSRB1* in the wild relative's defense against herbivore challenge. To assess the enzymatic properties of *Cp*MSRB1, the gene was overexpressed in-frame with maltose-binding protein (MBP) in the *Escherichia coli* BL21-CodonPlus strain and purified using immobilized amylose (Supplementary Fig. S1A to C). The catalytic ability of purified *Cp*MSRB1 was evaluated through in vitro reduction of dabsylmethionine sulfoxide (dabsyl-Met-SO) to dabsyl-Met in the presence of dithioerythritol (DTE) using high-performance liquid chromatography (HPLC) (Fig. 2B). In the presence of *Cp*MSRB1, peaks corresponding to dabsyl-Met-SO and dabsyl-Met were detected at approximately 12.3 and 14.3 min, respectively (Fig. 2B). However, in the absence of *Cp*MSRB1, a single peak of dabsyl-Met-SO was observed at around 12.3 min (Fig. 2C). Further, *Cp*MSRB1 was found to exhibit substantial activity under the standardized HPLC conditions (Fig. 2D). Subsequently, the substrate stereospecificity of *Cp*MSRB1 was determined using a specific HPLC program (Fig. 2E and F). Without *Cp*MSRB1, overlapped peaks representing stereoisomers of dabsyl-Met-SO (dabsyl-Met-S-SO and dabsyl-Met-R-SO) indicated the absence of reduction activity and the presence of both isomers. However, in the presence of *Cp*MSRB1, a peak for dabsyl-Met was detected at approximately 25.9 min, signifying MSR activity. Further, a reduction in the peak area for dabsyl-Met-R-SO confirmed the stereospecificity of *Cp*MSRB1 (Fig. 2E and F).

*Cp*MSRB1 physically interacts and repairs chorismate mutase (*Cp*CM1.1), a pivotal enzyme in the phenylpropanoid pathway essential for sustained polyphenol production during herbivory

MSR proteins are known for their role in the repair of redox proteins involved in cellular ROS scavenging (Cui et al. 2022; Ding et al. 2021; Hazra et al. 2022; Hu et al. 2023; Xiao et al. 2021; Zhao et al. 2022). We wanted to identify the plausible protein substrate interacting with *Cp*MSRB1 in the present study. For this, a high-quality yeast (Y187 strain) prey library (3×10^7 CFU/ml colonies) from *H. armigera*-challenged *C. platycarpus* samples was mated with *Cp*MSRB1 as the bait protein in the Y2HGold strain. Screening of *Cp*MSRB1-interacting proteins on DDO (double dropout)/X-α-gal plates led to the identification of six blue colonies (B1 to B6), which were further plated on DDO/X-α-gal/aureobasidin A (AbA) and QDO (quadruple dropout)/X-α-gal/AbA (Supplementary Fig. S2A). We followed stringent screening and selected those colonies that survived on QDO media with X-α-gal and AbA (200 ng/ml). As provided in Supplementary Figure S2A, because B2 and B3 colonies could not survive, we proceeded with sequencing of the remaining four prey plasmids (B1, B4, B5, and B6). The resulting sequences were aligned against *C. cajan* proteins using NCBI protein BLAST and E values provided accordingly. Out of the four colonies, B4 could grow quickly and covered the entire streaked area on the plate, whereas others took a comparatively longer time to grow. Considering the pace of growth, as well as biological relevance to the present study, we went ahead with B4 (chorismate mutase: *Cp*CM1.1) (Supplementary Fig. S2B). Subsequently, the presence of a chorismate mutase domain in the selected prey protein confirmed its identity (Supplementary Fig. S3). The proof of interaction between *Cp*MSRB1 and *Cp*CM1.1 was additionally obtained in vivo in yeast (Fig. 3A) and in planta through a bimolecular fluorescence complementation (BiFC) assay in *Nicotiana benthamiana* (Fig. 3B). A *Cp*MSRB1-*Cp*CM1.1 complex was seen to be formed in the

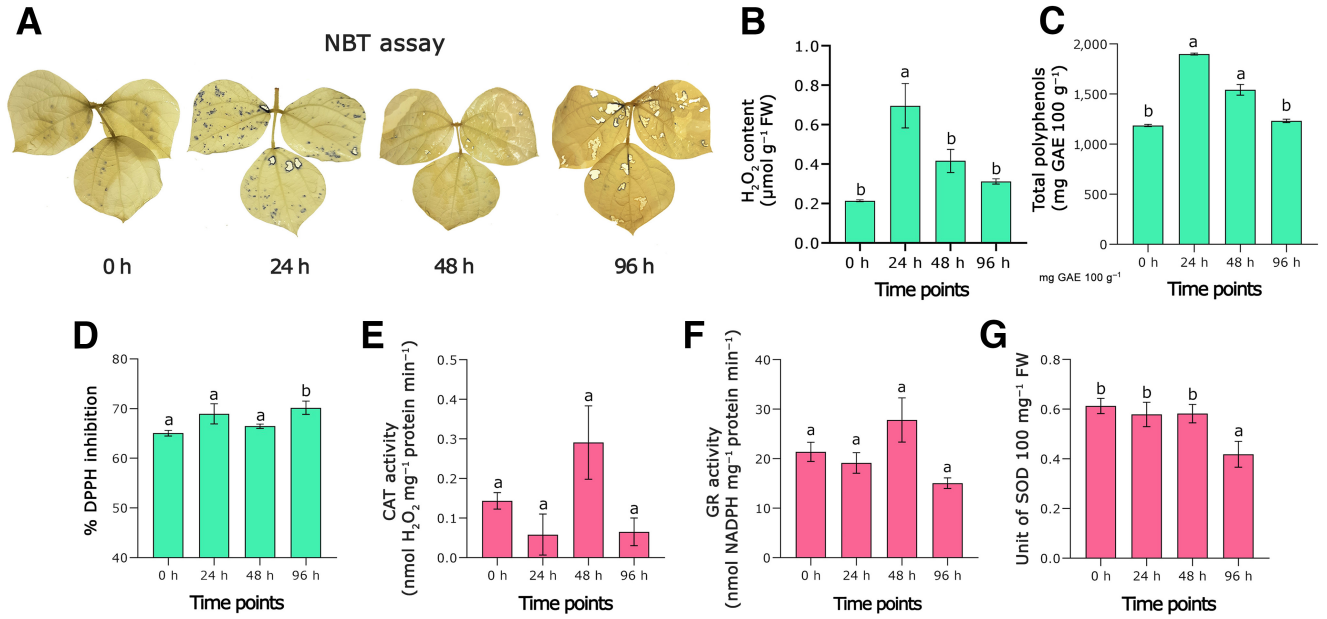

Fig. 1. Reactive oxygen species management in *Cajanus platycarpus* under continued herbivory by *Helicoverpa armigera*. **A,** Nitroblue tetrazolium (NBT) staining of *C. platycarpus* leaves collected at different time points of herbivore feeding. **B,** Spectrophotometric measurement of H_2O_2 in *C. platycarpus* leaves under continued herbivory. **C,** Alteration in total polyphenol content in the wild relative at different time points of herbivory. **D,** Bar graph representation of free radical scavenging capacity (2,2-diphenyl-1-picrylhydrazyl [DPPH]) under continued herbivory in *C. platycarpus*. **E to G,** Assessment of catalase (CAT), glutathione reductase (GR), and superoxide dismutase (SOD) activities, respectively, at different time points of herbivory in the wild relative. Data represent mean ± SE of four biological replicates. Different letters indicate significant differences in means determined using one-way analysis of variance with Duncan's multiple range test ($\alpha = 0.05$). FW, fresh weight.

chloroplast, as depicted through BiFC (Fig. 3B). Additional support for the BiFC assay was obtained by western blot analysis that confirmed the expression of full-length *Cp*MSRB1-c-Myc-nYFP and *Cp*CM1.1-HA-cYFP proteins (Supplementary Fig. S4).

This result encouraged us to further investigate whether the methionine-rich *Cp*CM1.1 enzyme was susceptible to sulfoxide modifications, which are subsequently repaired by *Cp*MSRB1 (Fig. 3C). To verify this possibility, the recombinant protein of *Cp*CM1.1 was overexpressed in *E. coli* and purified as described in the previous section (Supplementary Fig. S1D to F). The purified *Cp*CM1.1 was then subjected to H_2O_2 treatment for oxidization. Accordingly, a shift in the molecular weight of the purified recombinant *Cp*CM1.1 to a higher size due to oxidation of methionine residues was observed in the presence of H_2O_2. However, upon the addition of *Cp*MSRB1, the shift in protein molecular weight of *Cp*CM1.1 was not observed despite the presence of H_2O_2, similar to control conditions (*Cp*CM1.1, *Cp*CM1.1 + *Cp*MSRB1; Fig. 3C). These results were also validated by western blot using anti-c-Myc antibodies against *Cp*CM1.1 tagged with c-Myc epitope (Fig. 3C). Based on these findings, we further validated *Cp*CM1.1 as the key interacting partner responsible for ROS homeostasis-mediated defense response in the wild relative, which thus warranted further investigation.

*Cp*CM1.1, the identified substrate of *Cp*MSRB1, is herbivore-responsive in *C. platycarpus*

We wanted to check whether chorismate mutase, the identified MSR substrate, was indeed herbivore responsive. Based on the in-house-generated transcriptome data (Rathinam et al. 2019), four *CpCM* isoforms (*CpCM1*, *CpCM1.1*, *CpCM2*, and *CpCM3*) were identified. qRT-PCR analysis revealed a discrete response of these genes to herbivory (Fig. 3D). Whereas *CpCM3* showed up to -1.5 $\log_2$ fold change downregulation, *CpCM1* and *CpCM2* showed a slight change in expression, which was, however, not significant. Nevertheless, *Cp*CM1.1 identified as the *Cp*MSRB1 substrate through yeast two-hybrid (Y2H) experiments showed significant herbivore-responsive expression. A gradual rise from the initial time point of herbivory was seen that reached 1.7-fold increased expression by 96 h (Fig. 3D). The differential response of *CpCM1.1* to herbivory justified the specific *Cp*CM1.1-*Cp*MSRB1 interaction. Comparison of the *Cp*CM1.1 sequence with the other isoforms revealed 70% similarity with *Cp*CM1, 61% with *Cp*CM3, and 47% with *Cp*CM2 (Supplementary Fig. S5). This implied distinctness across the isoforms and probable sequence-specific interaction between *Cp*MSRB1 and *Cp*CM1.1.

To further validate the interaction between *Cp*MSRB1 and *Cp*CM1.1, high-quality structures were modeled (Supplementary Fig. S6) before performing docking analysis. For this, the top 10 docking poses were predicted using the HDOCK server, and the best docked pose obtained an HDOCK score of −158.09. In the case of *Cp*MSRB1, the two loop region residues (116 to 121 and 165 to 172) between the antiparallel β-strands that formed the active site of the protein were found to interact with the *Cp*CM1.1 protein (Fig. 4A and B). Subsequent analysis was conducted to delineate the interaction between *Cp*MSRB1 and *Cp*CM1.1. Accordingly, the docking study showed potential

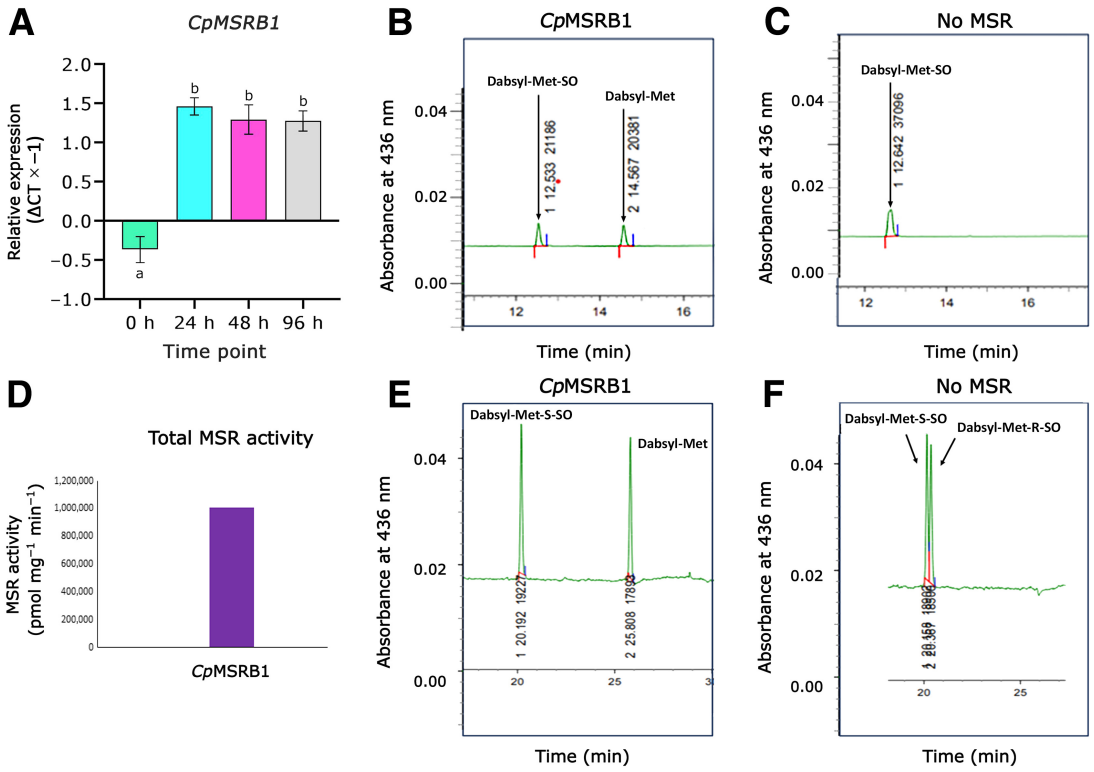

Fig. 2. Expression analysis and biochemical characterization of *Cp*MSRB1. **A,** Gene expression analysis of *CpMSRB1* at different time points of herbivory in *Cajanus platycarpus*. For ease of interpretation, relative expression is presented as ΔCT × −1; higher values are considered upregulation, and lower are considered downregulation. Data represent mean ± SE of four biological replicates. Different letters indicate significant differences in means determined using one-way analysis of variance with Duncan's multiple range test ($\alpha = 0.05$). **B,** In vitro reduction of dabsylmethionine sulfoxide (dabsyl-Met-SO) to dabsyl-Met in the presence of *Cp*MSRB1 showed dabsyl-Met-SO and dabsyl-Met peaks at approximately 12.3 and 14.3 min, respectively. **C,** Absence of *Cp*MSRB1 in the reaction produced no peak for dabsyl-Met. **D,** Total *Cp*MSRB1 activity as determined by high-performance liquid chromatography (HPLC). Program 1 was used to determine total methionine sulfoxide reductase (MSR) activity. **E,** HPLC-based detection of *Cp*MSRB1 substrate specificity as determined by the reduction of dabsyl-Met-R-SO to dabsyl-Met. Only in the presence of *Cp*MSRB1 was a peak corresponding to dabsyl-Met observed at 25.9 min. **F,** HPLC-based demonstration of the presence of both the stereo isoforms, dabsyl-Met-R-SO and dabsyl-Met-S-SO, in the absence of recombinant *Cp*MSRB1.

interactions resulting in the formation of hydrogen bonds (Fig. 4B; Supplementary Table S1). Notably, amino acid residues ASN-146, ASN-147, ALA-167, ASP-170, and LYS-198 of *Cp*MSRB1 were predicted to interact with *Cp*CM1.1. Further, ASP-121 and ASP-170 of *Cp*MSRB1 possessed electrostatic interactions toward ARG-150, LYS-161, and ARG-14 of *Cp*CM1.1, respectively (Fig. 4B). Overall, docking results revealed that amino acid residues in the adjoining region and within the catalytic motifs (CXXC and RXCXNS) of *Cp*MSRB1 were found to interact with *Cp*CM1.1. Meanwhile, the C-terminal

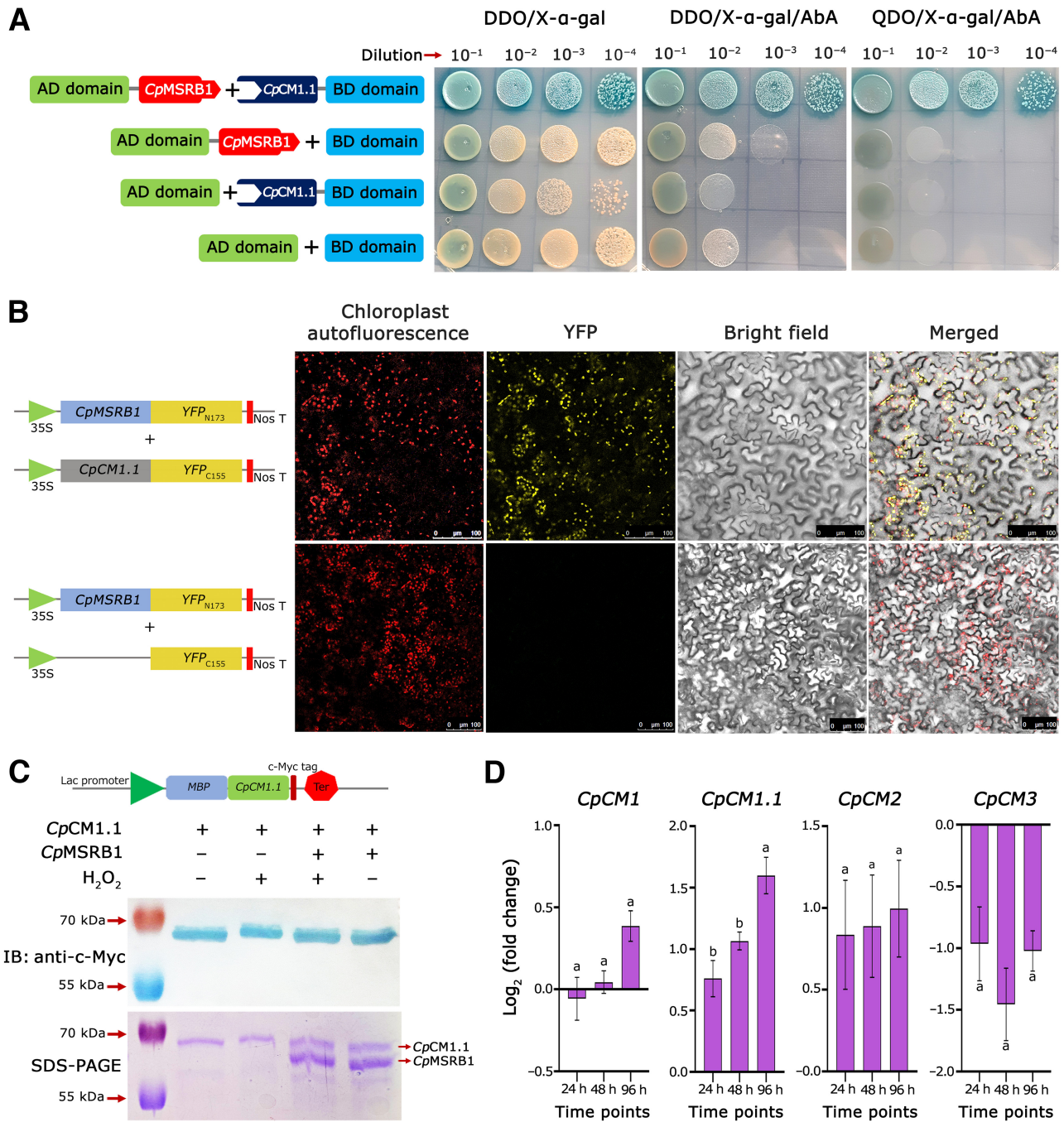

Fig. 3. Identification and validation of *Cp*MSRB1-interacting partner in the wild relative in response to herbivory. **A,** Assessment of *Cp*MSRB1-prey protein interaction by screening on three different media: double dropout (DDO, –Leu, –Trp)/X-α-gal, DDO/X-α-gal/aureobasidin A (AbA), and quadruple dropout (QDO; –Ade, –His, –Leu, –Trp)/X-α-gal/AbA. Yeast two-hybrid (Y2H) interactions were performed with four different combinations of prey and bait plasmids transformed into the Y2HGold strain: (i) AD domain::*Cp*MSRB1 + BD domain::*Cp*CM1.1; (ii) AD domain::*Cp*MSRB1 + BD domain; (iii) AD domain + BD domain::*Cp*CM1.1; and (iv) AD domain + BD domain. **B,** Bimolecular fluorescence complementation (BiFC) assay for the validation of *Cp*MSRB1-*Cp*CM1.1 interaction in *Nicotiana benthamiana.* For the BiFC assay, *N. benthamiana* leaves were co-infiltrated with pSPYNE173::*CpMSRB1-eYFP*$_{N173}$ and pSPYCE(M)::*CpCM1.1-eYFP*$_{C155}$ plasmids. For the negative control, pSPYNE173::*CpMSRB1-eYFP*$_{N173}$ and pSPYCE(M)::*eYFP*$_{C155}$ plasmids were used. After 24 h, the fluorescence signal was recorded through the yellow fluorescent protein (YFP) channel, and autofluorescence of chloroplasts was recorded in the respective fluorescence channel. **C,** In vitro Met-SO modification and repair assay of purified recombinant *Cp*CM1.1 (with c-Myc-epitope tag) protein through SDS-PAGE and immunoblotting (IB) using anti c-Myc antibodies. **D,** Gene expression analyses of *CpCM* isoforms (*CpCM1*, *CpCM1.1*, *CpCM2*, and *CpCM3*) in *Cajanus platycarpus* under continued herbivory. *Initiation factor 4α* was used as an internal control. Log_2 fold change was calculated with 0 h (unchallenged) as the baseline. Data represent mean ± SE of four biological repeats. Different letters indicate significant differences in means determined using one-way analysis of variance with Duncan's multiple range test ($\alpha = 0.05$). Lac promoter, lactose promoter; MBP, maltose binding protein; Ter, terminator.

residues of *Cp*CM1.1 located in the catalytic domain and possessing nearby surface-exposed Met residues were also observed to interact with *Cp*MSRB1.

To gain insights into the dynamic nature of the protein-protein interaction, molecular dynamics simulations were performed. The docked complex was subjected to 100 ns of simulation in explicit water. Evaluation using the root mean square deviation demonstrated that the docked complex was well stabilized throughout the simulation period, with an average root mean square deviation of 0.5 nm (Fig. 4C). Root mean square fluctuation values calculated to assess the dynamic behavior of individual amino acid residues in complexes demonstrated not many fluctuations in the residues of the *Cp*MSRB1-*Cp*CM1.1 docked complex, whereas minor fluctuations were observed in the C-terminal region of the *Cp*CM1.1 protein (Fig. 4D).

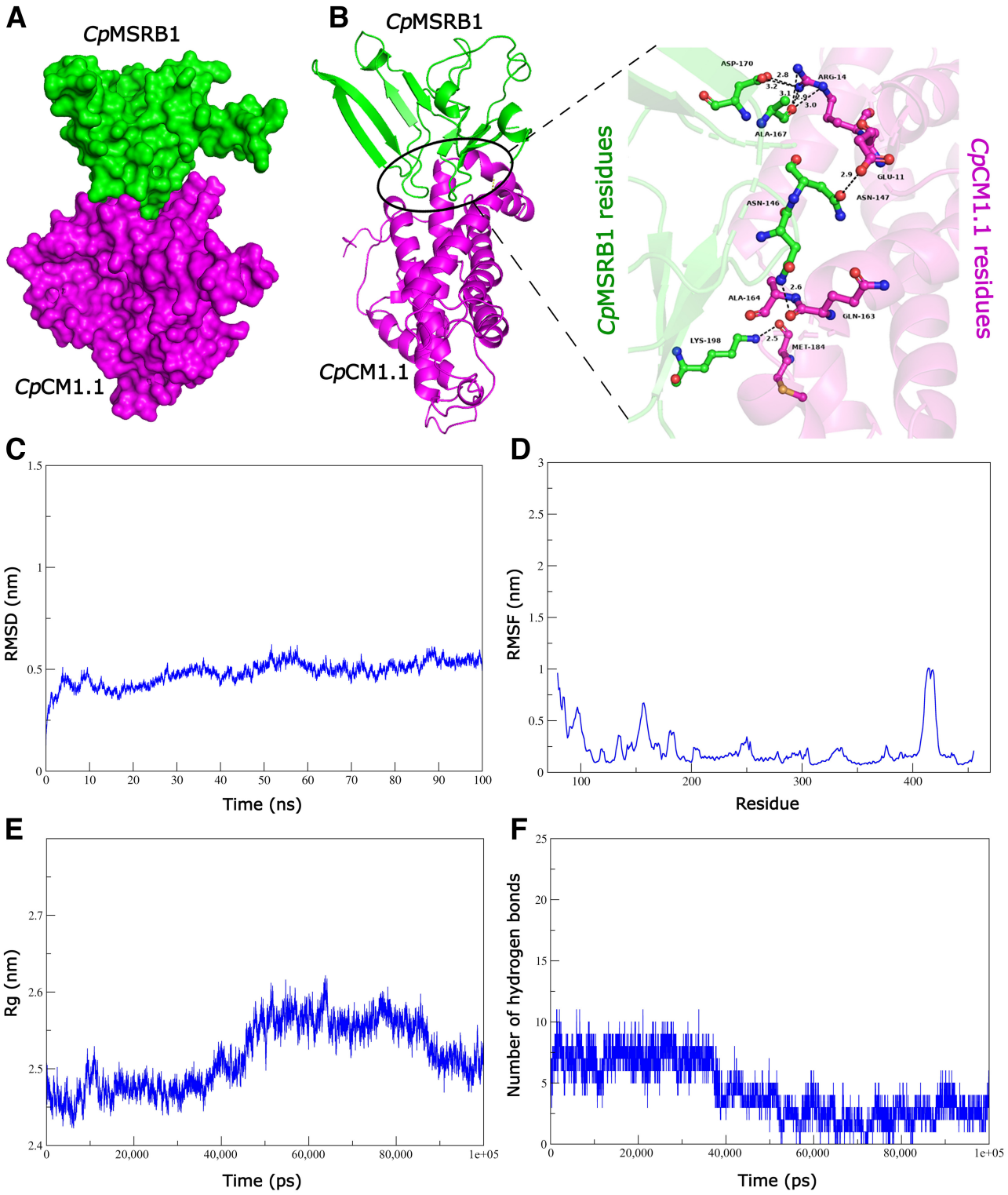

Fig. 4. In silico interaction analysis of *Cp*MSRB1-*Cp*CM1.1. **A and B,** Depiction of interactions between the predicted three-dimensional structures of *Cp*MSRB1 and *Cp*CM1.1. **C and D,** Root mean square deviation (RMSD) and root mean square fluctuation (RMSF) graphs of the *Cp*MSRB1-*Cp*CM1.1 interaction complex, respectively. **E and F,** Radius of gyration (Rg) graph and number of hydrogen bonds present in the docked complex, respectively.

The radius of gyration, a measure of the overall size and compactness of a biomolecule, provides valuable information about the conformational dynamics, stability, and structural changes of the system. The radius of gyration plot for the alpha (α) carbon atoms of the *Cp*MSRB1-*Cp*CM1.1 docked complex revealed an average compactness of 2.5 nm (Fig. 4E), suggesting that the docked complex remained stable and compact throughout the simulation period. To gain a deeper understanding of the atomic interactions within the *Cp*MSRB-*Cp*CM1.1 docked complex, we conducted analysis of hydrogen bonds forming the interface over a 100-ns simulation of the complex. Our findings revealed that docked complexes were stabilized by hydrogen bond interactions (Fig. 4F), with an average of five intermolecular hydrogen bonds exchanged by interface residues.

Repair of *Cp*CM1.1 by *Cp*MSRB1 in *C. platycarpus* during continued herbivory leads to a synergistic salicylic acid (SA)/jasmonic acid (JA)-mediated defense response

Traditionally, plant defense responses against insect herbivory are mediated by JA signaling (Shan et al. 2009; Ullah et al. 2023). An intriguing hypothesis regarding the potential role of SA in this system arose from our previous finding, which showed the accumulation of both JA and SA in the wild relative under sustained herbivory (Dokka et al. 2024). Furthermore, the evidence from this study that *Cp*MSRB1 repairs CM in the wild relative prompted us to conduct a more in-depth investigation. Importantly, CM is known to drive the phenylpropanoid pathway, which is responsible for SA biosynthesis. Whereas JA is produced through a multistep pathway, SA biosynthesis in plants originates from the shikimate pathway, which diverges from chorismate. One branch of this pathway is facilitated by *isochorismate synthase* (*ICS*), and the other branch is mediated by *CM*, followed by *phenylalanine ammonia-lyase* (*PAL*; Fig. 5A). Gene expression analysis revealed a gradual downregulation of *CpICS*, with ΔCT decreasing by up to −2 by 96 h of herbivore infestation compared with control conditions. Conversely, in the second branch, the expression of two *CpPAL* isoforms, namely *CpPAL2* and *CpPAL2.1*, exhibited a maximum upregulation of 2 and 3 ΔCT variation, respectively, by 96 h of herbivory (Fig. 5B). Furthermore, *abnormal inflorescence meristem1* (*CpAIM1*), another downstream gene

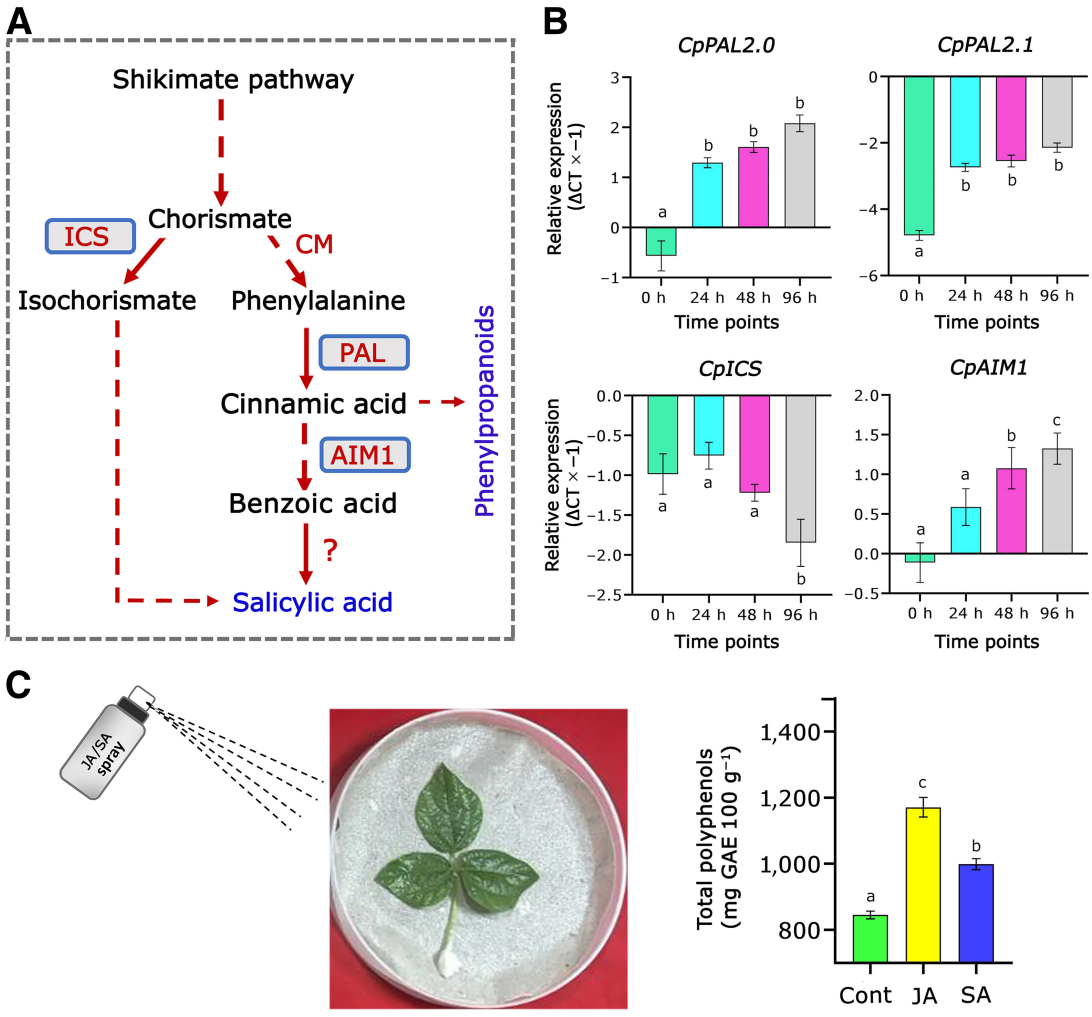

Fig. 5. Depiction of jasmonic acid (JA)- and salicylic acid (SA)-mediated defense response in *Cajanus platycarpus* during continued herbivory. **A,** Schematic representation of SA-producing pathways in plants. Blue boxes indicate key enzymes, and the dotted line indicates multiple steps involved in SA production. **B,** Gene expression analysis for the identification of the SA biosynthesis pathway being followed in *C. platycarpus* under herbivory. *PAL*, *phenylalanine ammonia lyase*; *ICS*, *isochorismate synthase*; *AIM1*, *abnormal inflorescence meristem 1*. For ease of interpretation, relative expression is presented as ΔCT × −1; higher values are considered upregulation, and lower are considered downregulation. **C,** Assessment of exogenous JA- and SA-mediated accumulation of total phenols in the pigeonpea wild relative. Data represent mean ± SE of four biological repeats. Different letters indicate significant differences in means determined using one-way analysis of variance with Duncan's multiple range test (α = 0.05). Cont, control.

within the second branch, also displayed upregulation, reaching up to 1.25 ΔCT variation (Fig. 5B). This demonstrated that SA was indeed being produced during the defense response in the wild relative and occurred through the chorismate pathway.

Additional proof for JA- and SA-mediated production of total phenols in the wild relative was demonstrated in the present study. Whereas the total phenol content in control sample was 850 mg gallic acid equivalent [GAE] 100 g^{-1}, JA- and SA-sprayed leaf samples accumulated up to 1,200 and 1,000 mg GAE 100 g^{-1}, respectively (Fig. 5C).

Heterologous expression of *CpMSRB1* in tomato demonstrated improved ROS management and reduced herbivore performance

The major objective was to validate the *CpMSRB1*-mediated ROS homeostasis in a heterologous system. For this, transgenic tomato plants over expressing the *CpMSRB1* gene under the control of the Enh-CaMV35S promoter were generated through *Agrobacterium tumefaciens*-mediated transformation of cotyledonary explants (Fig. 6A; Supplementary Fig. S7). Primary transformants that remained green and healthy after three rounds of kanamycin selection were advanced further. After stringent selection, eight T_0 tomato plants and vector control plants that showed healthy growth and phenotype were selected for efficacy analysis against *H. armigera*.

Initially, transgenic plants challenged with second instar *H. armigera* portrayed reduced leaf damage, and three plants, TP-6, TP-7, and TP-16, that exhibited <40% leaf damage were selected (Fig. 6B and C), whereas vector control plants showed >65% leaf damage. Larvae that fed on *CpMSRB1* transgenic tomato leaves exhibited growth reduction compared with those that fed on the vector control leaves (Fig. 6D).

Based on the ability of *CpMSRB1* transgenics to control pod borer feeding, TP-6, TP-7, and TP-16 were selected for molecular and biochemical analysis. The presence of *CpMSRB1* gene in the selected transgenic plants was confirmed by the amplification of a 700-bp CaMV35S promoter-gene-specific fragment (Fig. 6E). Further, integration of the selectable marker gene was also demonstrated by the amplification of a 750-bp *nptII* gene fragment (Fig. 6E).

To corroborate bioefficacy and integration analyses, we assessed the transcript level of *CpMSRB1* in transgenic tomato plants. Conclusive evidence in support of *CpMSRB1* integration in the transgenic plants was obtained by qRT-PCR analysis, which demonstrated expression of *CpMSRB1* in the selected events (Fig. 6F). Increased *CpMSRB1* transcript accumulation (four- to sixfold) was detected in all the transgenic plants that had earlier demonstrated superior efficacy against *H. armigera* challenge.

Transgenic tomato plants (TP-6, TP-7, and TP-16) and vector control plants were subsequently assessed for the ability to scavenge ROS during oxidative stress (Fig. 7). NBT staining of leaf samples collected before the stress, during oxidative stress imposition, and during the recovery period indicated increased accumulation of ROS in the vector control plants (Fig. 7A). However, there was a conspicuous reduction of ROS during the recovery period in the transgenic leaves when compared with oxidative stress-imposed leaves (Fig. 7A). Corroboratory evidence on the ability of transgenic tomato plants to better scavenge ROS was obtained upon the quantification of total phenols during oxidative stress and the recovery period when compared with the non-stress condition (Fig. 7B). TP-16 displayed the highest accumulation of total phenols under both stress and non-stress conditions (Fig. 7B). Further, a DPPH assay (Fig. 7C) also portrayed effective scavenging of antioxidants in tomato transgenics overexpressing *CpMSRB1*.

Discussion

Understanding how plants exhibit cellular level tolerance and maintain the expression of vital proteins under oxidative stress induced by insect herbivory is an important area of study. Efficient ROS scavenging serves as the first line of defense, preventing oxidative damage and maintaining cellular balance. This is especially important because plant defense against prolonged herbivory is energy-demanding, necessitating a shift in metabolic flux toward the production of defense metabolites and the activation of protective proteins and enzymes essential for survival (Erb and Reymond 2019; Gershenzon and Ullah 2022; Mithöfer and Boland 2012; Ullah et al. 2023). Therefore, understanding this phenomenon is crucial, especially in a plant with an inherent resistance to a specific herbivore. This study focused on *C. platycarpus*, which had previously been shown to strategically produce secondary metabolites (Rathinam et al. 2019, 2020; Tyagi et al. 2022a) and effective redox homeostasis (Rathinam et al. 2022) as a part of its defense response. Considering this agility of the wild relative, the current study was designed to understand in depth redox homeostasis during *H. armigera* challenge. Demonstration of an early and efficient removal of ROS during herbivory and the resulting rise in the overall phenol content aligned with our previous findings that showed downregulation of genes coding for crucial antioxidant enzymes (Rathinam et al. 2022). An early surge in ROS during the onset of herbivory is not only essential for defense activation but also apparently affects nutrient absorption in the insect midgut (Ahmad and Pardini 1990; Felton et al. 1992). The fact that the activity of key antioxidant proteins (CAT, SOD, and GR) was unaltered during herbivory further confirmed that *C. platycarpus* relied on non-enzymatic antioxidants for ROS scavenging. This non-canonical drift observed in *C. platycarpus* (Labudda et al. 2020) prompted us to further explore the defense response in the wild relative, focusing specifically on the management of ROS in response to continued herbivory.

MSRs are crucial enzymes that play a vital role in maintaining redox homeostasis (Rathinam et al. 2019, 2022). By reducing methionine sulfoxide back to methionine, they help protect cells from oxidative damage and regulate cellular responses to oxidative stress. Hence, they are mainly involved in the repair of functionally important cellular proteins (Brot and Weissbach 2000). Although the role and functional pathways of *MSR* genes have been well known in animal systems, only recently are they being highlighted in plants (Cui et al. 2022; Ding et al. 2021; Hazra et al. 2022; Xiao et al. 2021; Zhao et al. 2022). Our group previously demonstrated the functional relevance of these genes in the resistance response of *C. platycarpus* to herbivory (Rathinam et al. 2022). In this study, we conducted a detailed investigation on the role of the plastidial *CpMSRB1* in maintaining redox homeostasis. This led us to a question: could there be a link between increased phenolic content, redox balance, and the master regulator *Cp*MSRB1? The first evidence of this relationship was observed in our previous study, where we identified the role of the plastidial *Cp*MSRB1 in the resistance response of *C. platycarpus* to sustained herbivory (Rathinam et al. 2022). The significance of plastidial MSRs in mitigating ROS has been projected across diverse crops under various stress conditions (Ding et al. 2021; Hazra et al. 2022; Vieira Dos Santos et al. 2005; Zhao et al. 2022).

After confirming the herbivore responsiveness and substrate specificity of *Cp*MSRB1, we shifted our focus to identifying its interacting partner in the wild relative. We made a striking discovery when we identified the MSR substrate to be chorismate mutase (*Cp*CM1.1), a pivotal enzyme in the shikimate pathway that facilitates conversion of chorismate to prephenate, leading to the production of aromatic amino acids, such as phenylalanine,

tyrosine, and tryptophan. These amino acids serve as building blocks for a plethora of essential plant metabolites, including phytohormones, lignin, flavonoids, and alkaloids vital for plant growth, development, and defense (Yokoyama et al. 2021). Additionally, the *chorismate mutase* gene is of particular interest because of its regulatory role in plant defense responses and immune signaling pathways. Hence, these results supported our hypothesis on the role of *Cp*MSRB1 in repairing enzymes responsible for polyphenol production. Although a myriad of plant protein classes have been identified as MSRB substrates encompassing antioxidant enzymes (Cui et al. 2022; Hazra et al. 2022; Xiao et al. 2021; Zhao et al. 2022) and RUBISCO (Cui et al. 2022), our study represents the first instance of an enzyme involved in the secondary metabolite pathway to be the substrate. Hence, we determined that the role of *Cp*MSRB1 in the wild relative was to protect *Cp*CM1.1 from oxidation and drive the

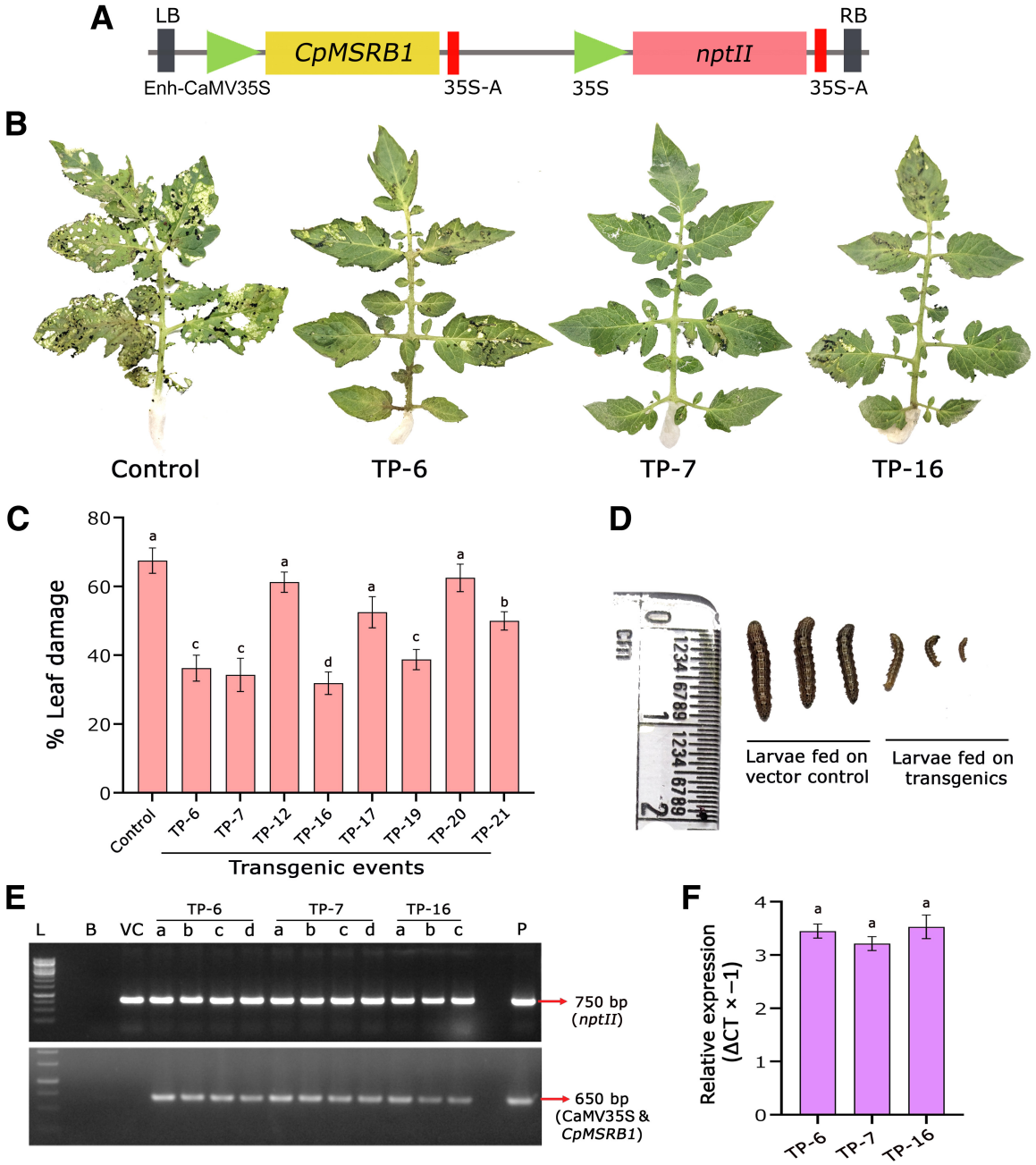

Fig. 6. Characterization of transgenic tomato plants (Pusa Ruby) overexpressing *CpMSRB1*. **A,** Schematic representation of the binary vector pCAMBIA2300 harboring *CpMSRB1*. The gene was cloned under the control of the CaMV35S promoter with enhancer and 35S polyA terminator. The selectable marker gene, *nptII*, was cloned under the control of the CaMV35S promoter and 35S polyA terminator (LB, left border; RB, right border). The binary vector was transformed into *Agrobacterium tumefaciens* strain GV3101 and used for tomato transformation. **B,** Bioefficacy analysis of transgenic tomato and vector control plants challenged with second instar *Helicoverpa armigera*. **C,** Graphical representation of the performance of individual *CpMSRB1* transgenic plants and vector control plants to deliberate challenge by *H. armigera*. **D,** Variation in the length of larvae that fed on transgenic tomato and vector control plants at the end of the detached leaf insect bioassay. **E,** PCR analysis of selected transgenic tomato plants for the amplification of a 750-bp *nptII* gene fragment and 650-bp CaMV35S promoter-*CpMSRB1* fragment. Lane, TP-6, TP-7, and TP-16–tomato transgenic events; L, 1-kb DNA ladder; B, template blank; VC, vector control; P, positive control (pCAMBIA2300::*CpMSRB1*). **F,** qRT-PCR analysis of selected transgenic events for the expression of the *CpMSRB1* gene. *Initiation factor 1* was used as an internal control gene, and ΔCT values were calculated using the difference in the CT mean of the target gene and the reference gene. Data represent mean ± SE of four biological repeats. Different letters indicate significant differences in means determined using one-way analysis of variance with Duncan's multiple range test ($\alpha = 0.05$).

flux toward the phenylpropanoid pathway for the sustained production of total phenols, the non-enzymatic ROS scavengers for self-sustenance and herbivore deterrence. This revelation not only asserted the expansive versatility of plant MSRs but also emphasized their crucial role in safeguarding essential proteins from oxidative damage.

We demonstrate that the ROS homeostasis-mediated defense response of *C. platycarpus* to *H. armigera* challenge is primarily driven by the sustained production of total phenols. Another intriguing question arose: considering the repair of chorismate mutase, does the wild relative opt for a direct and phenol-related route to SA production under stress, or does it take a more multifaceted approach? In plants, SA is produced through two pathways, one mediated by *ICS* and another by *CM*, followed by *PAL*. The *ICS* pathway is well characterized in model plants such as *Arabidopsis* (Ullah et al. 2023), whereas the second pathway involving *PAL* is longer and partially known. SA synthesis pathways diverge across plant species, with some relying on the *PAL* pathway under biotic stress conditions (Ullah et al. 2023; Xiao et al. 2021). In our study, conclusive evidence from the expression analyses of pathway genes highlighted the induction of *PAL*-dependent SA biosynthesis during insect herbivory in *C. platycarpus*. This discovery emphasized a captivating and a strategic redirection of metabolic flux into the phenylpropanoid pathway. Further, it also explained the reason behind the focused repair of *Cp*CM1.1 by *Cp*MSRB1.

This brought up another question: does this mean that the wild relative executed JA- and SA-mediated defense against the attacking herbivore? In plants, the two phytohormones JA and SA regulate defense signaling under biotic stress conditions and also regulate ROS scavenging through the induction of antioxidant enzymes and secondary metabolites (Shan et al. 2009; Ullah et al. 2023). Generally, herbivore response in plants is mediated by JA (Erb and Reymond 2019), whereas the role of SA is predominant in microbial infection (Ullah et al. 2023). Ideally, the metabolic fate of ROS signaling depends on the type of stress encountered (Bari and Jones 2009; Bürger and Chory 2019; Foyer and Noctor 2005) as identified in plants. Biotrophic pathogens promote SA accumulation via *NPR1* and *WRKY*s, whereas necrotrophic pathogens and chewing herbivores activate JA/ethylene pathways, favoring phenolic and lignin biosynthesis through *MPK3/6* and *ERF*s. Phloem-feeding insects mimic biotrophic attack, triggering SA responses. However, abiotic stresses such as drought and UV drive flavonoid

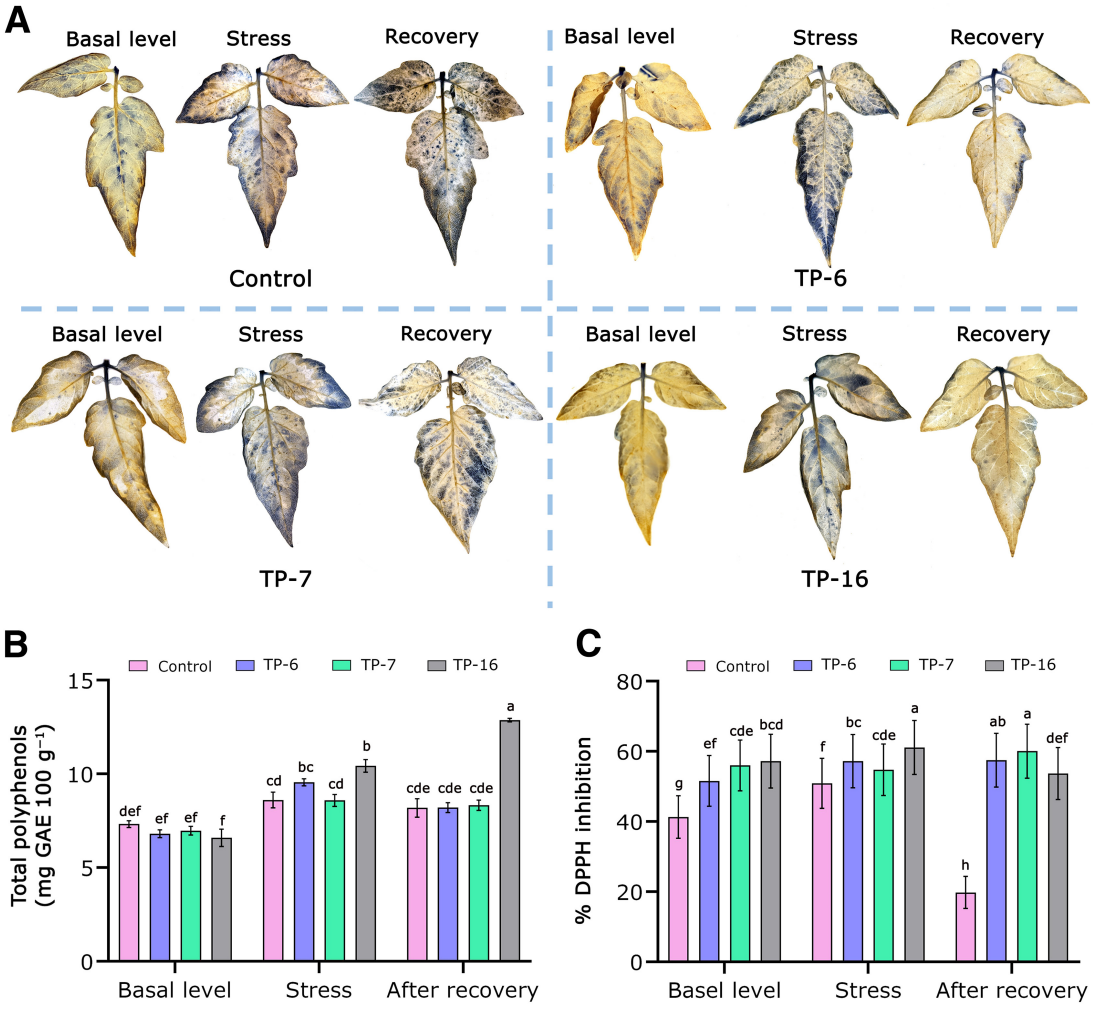

Fig. 7. Biochemical characterization of transgenic tomato plants harboring *CpMSRB1*. Oxidative stress was induced by exposing the selected transgenic and vector control plants to direct sunlight (approximately 120,000 lux) for 30 min followed by recovery for 30 min in the shade. Leaf samples were collected from the plants after stress as well as after recovery. **A,** Nitroblue tetrazolium (NBT) staining to assess reactive oxygen species (ROS) accumulation in selected tomato *CpMSRB1* transformants vis-à-vis vector control during basal level, oxidative stress, and post-recovery. **B,** Total polyphenol content in selected tomato *CpMSRB1* transformants vis-à-vis vector control during non-stress, oxidative stress, and post-recovery, respectively. **C,** Free radical scavenging activity in selected tomato *CpMSRB1* transformants vis-à-vis vector control during non-stress, oxidative stress, and post-recovery, respectively. Data represent mean ± SE of four biological repeats. Different letters indicate significant differences in means determined using one-way analysis of variance with post-hoc Tukey honestly significant difference test ($\alpha = 0.05$).

accumulation via *SnRK1* and *MYB* factors for ROS scavenging. These context-dependent shifts highlight the potential to engineer ROS-sensitive regulators to fine-tune metabolic flux and enhance stress-specific plant resilience. Furthermore, studies also reported an antagonistic role of JA and SA, triggered by effector molecules from pests (Ullah et al. 2023).

Interestingly, in *C. platycarpus*, we observed not only *PAL*-mediated production of SA but also accumulation of both SA and JA in response to continued herbivory (Dokka et al. 2024). These results highlight a collaborative pattern observed in *C. platycarpus* following insect herbivory. The cooperative interaction between JA and SA in plant defense is an uncommon occurrence, documented in just a handful of plant species (Ullah et al. 2023). This observation highlights a unique interaction between phytohormones in wild species, enabling the activation of metabolic responses—particularly noteworthy as both the JA and SA signaling pathways are linked to the biosynthesis of phenylpropanoids and flavonoids (Gondor et al. 2016; Shan et al. 2009; Singh 2023).

Furthermore, several studies have uncovered proteins that safeguard lipids from oxidative damage and thereby influence oxylipin and JA biosynthesis (Wasternack and Strnad 2019). Glutathione peroxidases, including phospholipid hydroperoxide glutathione peroxidases, reduce lipid hydroperoxides, limiting their conversion into JA precursors via the lipoxygenase pathway. Peroxiredoxins are known to detoxify peroxides, preventing excessive lipid oxidation, whereas aldo-keto reductases reduce oxidized lipid derivatives, fine-tuning JA signaling. Fatty acid hydroxylases and epoxygenases further modify oxidized fatty acids, reducing their reactivity and controlling jasmonate accumulation. By regulating the balance between lipid peroxidation and oxylipin production, these proteins determine the extent of JA-mediated defense responses. Engineering these lipid-protective mechanisms could allow for precise control over JA accumulation, mitigating growth-defense trade-offs in crops.

Having established the significance of *Cp*MSRB1 and identified its substrate during continued herbivory, it was crucial for us to validate this gene. To this end, overexpressing *CpMSRB1* in a heterologous system would offer insights into its impact on defense response against *H. armigera*. Remarkably, transgenic tomato plants with the introgressed *CpMSRB1* gene displayed enhanced resistance when faced with *H. armigera* larvae, surpassing control plants. Furthermore, this heightened resistance corresponded with increased levels of total phenols in these plants, emphasizing their improved performance against the attacking pest. Additionally, the transgenic plants showcased proficient ROS scavenging capabilities, further accentuating the importance of *Cp*MSRB1 in maintaining redox homeostasis during periods of stress.

Based on the information generated, a key avenue for future research would involve dissecting the molecular interaction between *Cp*MSRB1 and *Cp*CM1.1 to establish its precise role in ROS homeostasis and herbivore resistance. Targeted mutagenesis of *Cp*MSRB1 at its interaction sites with *Cp*CM1.1 could reveal whether the loss of binding abolishes its protective function against oxidative stress and, consequently, its ability to mitigate herbivore damage. Testing this in a heterologous system would provide compelling molecular evidence linking *CpMSRB1*, *CpCM1.1*, and ROS detoxification in plant defense. Additionally, an exciting possibility is engineering *Cp*MSRB1 variants with altered substrate specificity, enabling targeted ROS protection for specific cellular components or stress conditions. Such modifications could enhance plant resilience against oxidative stress and insect herbivory, paving the way for novel strategies in crop protection and stress adaptation.

In conclusion, we propose a model showcasing cellular activities in the wild relative in response to herbivory (Fig. 8). Accordingly, the onset of herbivore feeding initially resulted in the surge of ROS within the cell. To achieve ROS homeostasis for continued cellular function and herbivore deterrence, the plant primarily upregulated the plastidial *CpMSRB1*. This in turn physically interacted and repaired the plastidial *Cp*CM1.1, the gatekeeper of phenylpropanoid pathway, catalyzing a crucial step to direct the metabolic flow toward the biosynthesis of phenylalanine, SA, and, subsequently, the defense metabolites. Intriguingly, the active flux toward the phenylpropanoid pathway also stabilized SA production and its involvement in defense response, along with the canonical JA-mediated signaling due to herbivory. Therefore, uncovering the molecular basis of the wild relative's response to herbivory paves the way for new approaches in pest management and metabolic engineering. This research not only illuminated intricate defense mechanisms in plants but also emphasized the untapped potential of crop wild relatives in augmenting agricultural resilience, thereby offering promising solutions for sustainable agriculture in the face of evolving environmental challenges.

Materials and Methods

Plant material and deliberate herbivory by *H. armigera*

Seeds of *C. platycarpus* (ICPW068) were procured from the International Crops Research Institute for the Semi-Arid Tropics, Hyderabad, India. The seeds were sown in soil and maintained under net house conditions. *H. armigera* larvae collected from pigeonpea fields at the Indian Agricultural Research Institute, New Delhi, India, were reared in an insect culture room (26 ± 2°C, 70 ± 10% RH, and 16-/8-h light and dark photoperiod) on a chickpea-based artificial diet. Forty-five-day-old plants were challenged with second instar larvae of *H. armigera* as described in our previous studies (Rathinam et al. 2022; Tyagi et al. 2022a). The deliberate challenge with the herbivore was performed in four biological replicates at three different time points (24, 48, and 96 h), and untreated leaves were considered as 0 h. All the leaves were collected in liquid nitrogen and stored at −80°C until use.

Biochemical profiling to evaluate redox regulation in *C. platycarpus* amid persistent herbivory by *H. armigera*

NBT staining for O_2• detection. The production of free radicals in the leaves of the wild relative in response to herbivory was assessed by NBT staining. Leaves (four biological replicates) collected at different time points of herbivore challenge, along with unchallenged ones, were selected and subjected to staining following the standardized protocol (Juszczak and Baier 2014). Subsequent to staining, leaves were bleached using ethanol/acetic acid/glycerol in a 3:1:1 ratio overnight for visualization of blue formazan crystals indicating superoxide accumulation.

Hydrogen peroxide measurement. Hydrogen peroxide produced under continued herbivory was measured in leaf tissues of the wild relative collected at various time points of herbivore challenge using the potassium iodide method (Alexieva et al. 2001). For spectrophotometric quantification, the absorbance was recorded at 390 nm, and absolute concentration was calculated by a standard curve for H_2O_2 and expressed in μmol g^{-1} fresh weight.

Estimation of total phenol content. The challenged leaf tissues collected at different time points were used for the estimation of total phenol content. The extraction of phenolic compounds was carried out according to the standardized method (Emmons and Peterson 2001) with slight modifications. In brief, 100 mg of leaf tissue was ground in liquid nitrogen and mixed with 2 ml of 80% acidified methanol (1 ml of 1% HCl/80 m; of absolute methanol/9 ml of double-distilled H_2O). Subsequently,

it was kept at 25°C in an incubator (300 rpm) shaker overnight, followed by centrifugation at 10,000 rpm for 10 min, and filtered through Whatman No. 1 paper.

The total phenolic content was estimated using the Folin-Ciocalteu method (Singleton et al. 1999). Methanolic extracts (250 µl) and distilled water (1 ml) were mixed in a test tube, followed by the addition of Folin-Ciocalteu reagent (2 N; 250 µl). After a 6-min reaction, 2.5 ml of 7% Na_2CO_3 was added, the reaction mixture was incubated at room temperature for 90 min, and absorbance was recorded at 760 nm. A standard curve of gallic acid (Sigma-Aldrich, St. Louis, MO, U.S.A.) was prepared for the calculation of total phenols, and the results were expressed as milligrams of GAE per 100 g of tissue (mg GAE 100 g^{-1} tissue).

Estimation of DPPH radical scavenging activity. Approximately 100 mg each of herbivore-challenged and control leaf sample in four biological replicates was extracted in 2 ml of methanol by placing it on a shaker overnight. The extracts were later centrifuged at 10,000 rpm for 15 min. The assay was conducted following the standardized protocol (Mellors and Tappel 1966) using methanolic extracts with some modifications (Rathinam et al. 2022).

Analysis of SOD, CAT, and GR enzyme activities in *C. platycarpus*. Enzyme extracts for all the assays were prepared by grinding approximately 100 mg of leaf tissues from the wild relative collected at various time points of herbivory in 1 ml of 100 mM phosphate buffer (pH 7.5) containing 0.5 M EDTA (Sigma-Aldrich). The lysates were clarified at 15,000 g for 20 min at 4°C, and supernatants were used as an enzyme source. SOD (Dhindsa et al. 1981), CAT (Aebi 1984), and GR (Smith and Johnson 1988) activities were assessed through the respective standardized methods.

Bacterial overexpression, purification, and activity assessment of recombinant *Cp*MSRB1

The coding region of *CpMSRB1* was amplified from the cDNA of *C. platycarpus* using the Advantage 2 PCR Kit (Takara Bio, Shiga, Japan) with *Bam*HI (Thermo Fisher Scientific, Waltham, MA, U.S.A.) and *Hind*III (Thermo Fisher Scientific) sites. The fragment was further cloned into a pGEMT-easy vector

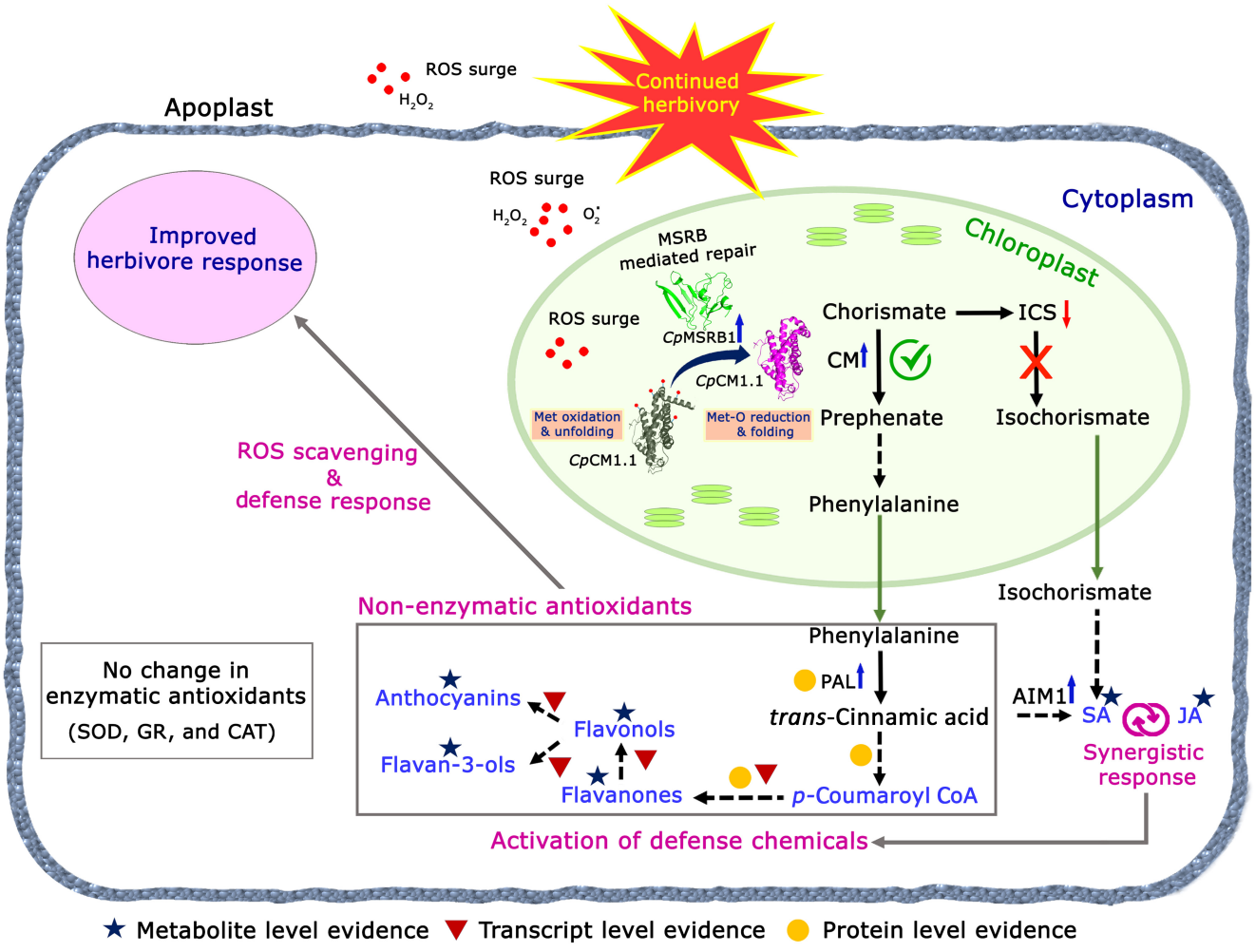

Fig. 8. Proposed model of reactive oxygen species (ROS) homeostasis in *Cajanus platycarpus* under *Helicoverpa armigera* attack. During herbivore infestation, a surge in ROS occurs across various cellular organelles, including the apoplast, cytoplasm, and chloroplast. In response, the pigeonpea wild relative strategically regulates ROS levels in the chloroplast by facilitating the repair of *CpCM1.1* through *CpMSRB1*, thereby redirecting metabolic flux toward phenylpropanoid biosynthesis. The evidence obtained in this study is represented in black font. Blue upward arrows indicate gene upregulation, and red downward arrows denote gene downregulation. Solid black arrows represent successive steps in the pathway, whereas dashed black arrows indicate multiple steps. Green arrows depict the movement of metabolites from the chloroplast to the cytoplasm. The induction of phenylpropanoids and their derivatives in response to sustained herbivory, as reported in our previous studies, is highlighted in blue font. Specific data sources are marked as follows: star symbols represent metabolome evidence (Dokka et al. 2024; Tyagi et al. 2022b); yellow circles indicate proteome evidence (Rathinam et al. 2020); and red triangles denote gene expression evidence (Rathinam et al. 2019; Tyagi et al. 2022b). Finally, conclusions derived from cumulative evidence across our studies and external research are depicted with gray arrows and pink font. JA, jasmonic acid; SA, salicylic acid; PAL, phenylalanine ammonia lyase; ICS, isochorismate synthase; AIM1, abnormal inflorescence meristem 1; SOD, superoxide dismutase; CAT, catalase; GR, glutathione reductase.

(Promega Corporation, Fitchburg, WI, U.S.A.) and confirmed through Sanger sequencing. For bacterial expression, *CpMSRB1* was sub-cloned into a pMALc2X vector (NovoPro, Shanghai, China) in-frame with MBP using *Bam*HI and *Hind*III sites, then mobilized into the BL21-CodonPlus strain (Agilent Technologies, Santa Clara, CA, U.S.A.). The protein induction was performed with 0.5 mM IPTG for 16 h at 24°C. The overexpressed proteins were purified using immobilized amylose (MBP resin; G Biosciences, Overland, MO, U.S.A.) as per the manufacturer's instructions.

MSR activity was assessed using dabsyl-Met (TCI Chemicals, Tokyo, Japan) as the substrate. For the preparation of dabsyl-Met-SO, 50 mM dabsyl-Met was incubated with 500 mM H_2O_2 at room temperature for 16 h, following the standardized protocol (Vieira Dos Santos et al. 2005). MSR activity was ascertained by examining the reduction of the synthetic substrate dabsyl-MetSO in the presence of the reducing agent DTE (Sigma-Aldrich), as optimized (Vieira Dos Santos et al. 2005), with minor modifications (Hazra et al. 2022). Furthermore, the analysis of total MSR activity and substrate stereospecificity of MSR proteins was performed through HPLC-based separation of dabsyl-MetSO and dabsyl-Met, respectively, utilizing specific standardized programs 1 and 2 (Vieira Dos Santos et al. 2005).

Y2H interaction analysis for the identification of *Cp*MSRB1-interacting partners

For the Y2H study, the full-length coding sequence of *CpMSRB1* was cloned into the pGBKT7 bait vector. The prey library was prepared from RNA samples of herbivore-challenged *C. platycarpus* as per the manufacturer's instructions (Takara Bio). The probable interacting partners of the bait protein were screened from the prey library by plating the mated culture on the DDO media (–Leu, –Trp) with X-α-gal and AbA. Positive clones obtained from the DDO media were further confirmed in QDO media (–Ade, –His, –Leu, –Trp) with X-α-gal and AbA as per the manufacturer's instructions (Matchmaker Gold Yeast Two-Hybrid System; Takara Bio).

Prey identification. All the positive yeast colonies obtained on QDO selection were subjected to colony PCR. Fragments with varying sizes were considered for further analysis. Prey plasmids were extracted from the selected yeast colonies and back-transformed into *E. coli* cells. Plasmids extracted from the bacterial clones were subjected to Sanger sequencing, and prey genes were confirmed through BLAST analysis.

Yeast 1 to 1 interaction. Prey proteins confirmed through the sequencing were further characterized by pairwise interaction. For this, individual prey plasmids, along with the pGBKT7:*CpMSRB1* plasmid, were respectively co-transferred into the Y2HGold strain (Takara Bio). The transformants were cultured on a DDO medium for 3 to 5 days and spotted on the DDO/X-α-gal, DDO/X-α-gal/AbA, and QDO/X-α-gal/AbA media with different dilutions: 10^{-1}, 10^{-2}, 10^{-3}, and 10^{-4}, followed by incubation for 3 to 4 days at 30°C.

BiFC assay

CpMSRB1 was cloned into the pSPYNE173 YFP-N-terminal vector (Waadt et al. 2008) using *Nco*I (Thermo Fisher Scientific) and *Xma*I (Thermo Fisher Scientific) sites, and one of the identified preys, *chorismate mutase* (*CpCM1.1*), was cloned into the pSPYCE (M) YFP-C-terminal vector (Waadt et al. 2008) using *Xba*I (Thermo Fisher Scientific) and *Xma*I (Thermo Fisher Scientific) sites. The cloned plasmids were individually transformed into *A. tumefaciens* strain GV3101 and co-infiltrated into *N. benthamiana* leaves for transient expression (Rathinam et al. 2019). The yellow fluorescent protein (YFP) signal was captured using a laser scanning confocal microscope (SP5; Leica, Wetzlar, Germany). Additionally, expression of both the individual full-length proteins in *N. benthamiana* was confirmed through immunoblotting using anti-c-Myc and anti-HA antibodies (Takara Bio).

Analysis of sulfoxide modification in the recombinant *Cp*CM1.1

The *CpCM1.1* gene was initially amplified with *Eco*RI (Thermo Fisher Scientific) and *Xba*I (Thermo Fisher Scientific) sites from the respective prey plasmid 'B4' using the Advantage 2 PCR Kit. Subsequently, a c-Myc epitope sequence was incorporated before the *Xba*I site in-frame with *CpCM1.1* using two sets of primers (Supplementary Table S2). The fragment was further cloned into a pGEMT-easy vector and authenticated through Sanger sequencing. The gene was successively subcloned into a pMALc2X vector in-frame with MBP using *Eco*RI and *Xba*I sites and mobilized into *E. coli* BL21-CodonPlus. For in vitro methionine sulfoxide modification analysis, recombinant *Cp*CM1.1 was primarily induced and purified as described earlier in the case of *Cp*MSRB1. The purified *Cp*CM1.1 (5 μg) was incubated with 30 mM H_2O_2 in a reaction volume of 50 μl. This incubation was carried out at 37°C for a duration of 2 h and 30 min, both with and without the addition of 5 μg of *Cp*MSRB1, along with HEPES (pH 8) and DTE (Sigma-Aldrich). The sulfoxide production in *Cp*CM1.1 following exposure to oxidative stress induced by H_2O_2 was assessed by both SDS-PAGE and western blot using anti-c-Myc antibodies (Takara Bio) (Hazra et al. 2022; Xiao et al. 2021).

In silico validation of *Cp*MSRB1-*Cp*CM1.1 interaction

Molecular modeling and validation. *Cp*MSRB1 and *Cp*CM1.1 were modeled for structure prediction using MODELLER (version 10.4). The crystal structure of the mammalian MSRB2 protein (PDBID: 2L1U) and *A. thaliana* chorismate mutase (PDBID: 4PPU) (https://www.rcsb.org/pages/about-us/index) were used as templates for modeling. The segments corresponding to residues 1 to 78 were absent in the template crystal structure (2L1U) due to inadequate electron density, prompting the removal of these corresponding residues from the query sequence before alignment. The resulting alignment was utilized to generate the model via MODELLER software (Šali and Blundell 1993) (version 10.4). The structure obtained from MODELLER underwent validation using the PROCHECK server (Laskowski et al. 2006).

Docking studies. To examine the possible interaction between *Cp*MSRB1 and *Cp*CM1.1, docking studies were performed using the modeled structures that were initially submitted to the HDOCK server (Yan et al. 2020). The most favorable docked complex was determined by selecting configurations with the lowest energy values and high docking scores. Analysis of the binding interactions within the interface of protein-protein complexes was then conducted using the PyMOL visualization tool (https://www.pymol.org/) (DeLano 2002), and interacting residues were identified.

Molecular dynamics simulation of the complex using GROMACS package. Molecular dynamics simulation was performed utilizing OPLS-AA/L all-atom force field to study interactions within the system (MacKerell et al. 1998; Van Der Spoel et al. 2005). The protein complex was placed in a cubic water box employing the Simple Point Charge (SPC 216) water model. Positioned at the center of the box and maintained 1.5 nm away from the box edge, the protein was subjected to periodic boundary conditions (Berendsen et al. 1981). For system neutrality, ions were introduced, substituting water molecules to ensure an overall charge balance of the protein complex. Steric clashes were mitigated through a rigorous energy minimization process involving 50,000 cycles utilizing the steepest descent algorithm. Subsequent equilibration stages were executed: NVT

equilibration, controlled by the Berendsen thermostat with a coupling time constant of 0.1 ps, and NPT equilibration, conducted using the Parrinello-Rahman barostat with a coupling constant of 2 ps (Berendsen et al. 1981; Parrinello and Rahman 1981). Maintaining bond lengths was facilitated by the linear constraint solver algorithm (Lincs) (Hess et al. 1997). Interactions, including Van der Waals and long-range electrostatic forces, were calculated utilizing the particle mesh Ewald electrostatics method, employing a Coulomb cutoff of 10 Å (Darden et al. 1993). The system underwent equilibration in two phases: initially with NVT ensembles, followed by NPT ensembles, each sustained for 100 ps. Subsequently, the finely balanced systems underwent a production run lasting 100 ns at 300 K and 1 bar pressure. This simulation employed a time step of 2 fs, with each conformation saved at regular intervals of 10 ps.

Effect of exogenous JA and SA on the total phenolic content in *C. platycarpus*

Healthy 45-day-old plants of the wild relative devoid of any insect pest attack and growing in the net house were selected for the experiment. For exogenous JA and SA treatments, detached trifoliate leaves were collected, placed in a Petri dish containing wet filter paper, and sprayed with a 2 mM solution of MeJA (Sigma-Aldrich) and 5 mM solution of SA (Sigma-Aldrich) prepared in distilled water containing 0.1% Triton X-100 (Sigma-Aldrich). The leaves without any spray were considered as absolute controls. The treated and untreated leaf tissues were collected in liquid nitrogen after 24 h and frozen at −80°C. Estimation of total phenols was carried out as described in the previous sections of the manuscript.

Gene expression analyses in *C. platycarpus*

Gene expression analyses for the assessment of accumulation of various transcripts were carried out by qPCR. Herbivore-challenged leaf samples were subjected to RNA extraction as per the manufacturer's instructions (Spectrum total RNA isolation kit; Sigma-Aldrich). cDNA synthesis was carried out using 2 µg of total RNA with the SuperScript VILO cDNA Synthesis Kit (Thermo Fisher Scientific). qRT-PCR was performed with gene-specific primers (Supplementary Table S2) using TB Green Premix Ex Taq II SYBR Green PCR Master Mix (Takara Bio) on the AriaMx Real-Time PCR system (Agilent Technologies), according to the manufacturer's instructions. The expression of the *Initiation factor 4*α (*IF4*α) gene in each sample was used for normalization (Sinha et al. 2015). qRT-PCR conditions were followed as standardized (Rathinam et al. 2019) and performed in four independent biological replicates with two technical replicates. The $\log_2$ fold change was calculated using the $2^{-\Delta\Delta CT}$ method (Livak and Schmittgen 2001). For relative expression, gene CT values were normalized using the reference CT value; ΔCT was calculated and provided as ΔCT × −1 for easier interpretation.

Functional characterization of *CpMSRB1* in the model plant tomato (Pusa Ruby)

CpMSRB1 (606 bp) was initially amplified from the cDNA of *C. platycarpus*, cloned into the pGEM-T Easy vector (Promega Corporation), sequence confirmed, and sub-cloned into the modified pCAMBIA2300 vector. The vector was further mobilized into *A. tumefaciens* strain EHA105 and used for the transformation of tomato (Pusa Ruby). For vector control, the explants were infected with *A. tumefaciens* strain EHA105 harboring the empty pCAMBIA2300 vector.

Regeneration and transformation of tomato. Cotyledonary explants were prepared for transformation following the standardized protocol (Sharma et al. 2009) with some modifications. In brief, surface-sterilized tomato seeds were grown on germination media containing half-strength Murashige and Skoog (MS) medium. Approximately 10-day-old seedlings were selected for cotyledonary explant preparation. The excised explants were pre-cultured on MS media containing B5 vitamins along with 2 mg/liter 6-benzylaminopurine (Sigma-Aldrich) for 48 h. The explants were then infected with an *Agrobacterium* suspension, followed by co-cultivation for 3 days on the same preculture medium. The explants were later transferred to a shoot initiation medium containing MS salts (1×) + Nitsch and Nitsch vitamins (1×; HiMedia Laboratories, Maharashtra, India) along with 1 mg/liter trans-zeatin (Sigma-Aldrich), 0.1 mg/liter indole acetic acid (IAA), 100 mg/liter kanamycin (HiMedia Laboratories), 250 mg/liter cefotaxime (HiMedia Laboratories), and 250 mg/liter carbenicillin (HiMedia Laboratories). Multiple shoots were excised, and individual shoots were transferred to a shoot elongation medium containing a B5 Gamborg medium (1×) along with 0.5 mg/liter trans-zeatin, 0.2 mg/liter IAA (Sigma-Aldrich), 100 mg/liter kanamycin, 250 mg/liter cefotaxime, and 250 mg/liter carbenicillin. Finally, well-elongated shoots were transferred to a rooting medium containing an MS B5 medium (1×; HiMedia Laboratories) along with 0.5 mg/liter IAA. Well-rooted plants were initially subjected to hardening in the culture room for 2 weeks and later transferred to the greenhouse.

Bioefficacy analysis of transgenic tomato plants harboring *CpMSRB1* to deliberate challenging by *H. armigera*. The efficiency of transgenic tomato plants harboring *CpMSRB1* against *H. armigera* challenge was assessed through a detached leaf insect bioassay. Healthy and well-established second or third leaves from 35- to 40-day-old *CpMSRB1* transgenic plants and vector control plants were collected for the bioassay. Five second instar *H. armigera* larvae, maintained on an artificial diet, were loaded onto each leaf. The insect bioassay was continued for 96 h, after which leaf damage and larval mortality were recorded. Percent damage was calculated based on the area of the leaf damaged by the larvae. The detached leaf bioassay was performed with three technical replicates each.

Molecular characterization of tomato transformants. High-quality genomic DNA for PCR analysis was isolated from tender leaves of tomato transformants following the cetyltrimethylammonium bromide (CTAB) method (Porebski et al. 1997). PCR analyses were performed using gene-specific and marker-specific primers (Supplementary Table S2). The reactions were carried out with approximately 100 to 150 ng of genomic DNA, and the reaction profile consisted of 30 cycles with denaturation at 94°C for 1 min, annealing (Supplementary Table S2) for 30 s, extension at 72°C for 1 min, and a final extension at 72°C for 10 min. PCR products were electrophoresed on a 0.8% agarose gel containing ethidium bromide and visualized under ultraviolet light.

The expression analysis of the *CpMSRB1* gene in tomato transgenics was performed as described earlier in the methods section, using *CpMSRB1*-specific primers and the *elongation factor 1* (*EF1*) gene for normalization (Supplementary Table S2). For relative expression, CT values were normalized using the reference CT value; ΔCT was calculated and provided as ΔCT × −1 for easier interpretation. The standard deviation between the replicates was calculated, and error bars were included.

Biochemical characterization of transgenic tomato plants. The selected *CpMSRB1* transgenic tomato and vector control plants were analyzed for their ability to control ROS through various biochemical assays. For this, oxidative stress was induced by exposing the selected transgenic and vector control plants to direct sunlight (approximately 120,000 lux) for 30 min followed by recovery for 30 min in the shade. Leaf samples were collected from the plants after stress as well as after recovery.

Total phenol content, DPPH activity, and NBT staining were carried out as previously described in the methods section.

Acknowledgments

Manoj Kumar is acknowledged for the maintenance of *C. platycarpus* and transgenic tomato plants and Vinod Kumar for the rearing and maintenance of *H. armigera*.

Literature Cited

Aebi, H. 1984. Catalase *in vitro*. Methods Enzymol. 105:121-126.

Ahmad, S., and Pardini, R. S. 1990. Mechanisms for regulating oxygen toxicity in phytophagous insects. Free Radical Biol. Med. 8:401-413.

Alexieva, V., Sergiev, I., Mapelli, S., and Karanov, E. 2001. The effect of drought and ultraviolet radiation on growth and stress markers in pea and wheat. Plant Cell Environ. 24:1337-1344.

Ali, S., Tyagi, A., and Bae, H. 2023. ROS interplay between plant growth and stress biology: Challenges and future perspectives. Plant Physiol. Biochem. 203:108032.

Bari, R., and Jones, J. D. G. 2009. Role of plant hormones in plant defence responses. Plant Mol. Biol. 69:473-488.

Berendsen, H. J. C., Postma, J. P. M., van Gunsteren, W. F., and Hermans, J. 1981. Interaction models for water in relation to protein hydration. Pages 331-342 in: Intermolecular Forces. B. Pullman, ed. Proceedings of the Fourteenth Jerusalem Symposium on Quantum Chemistry and Biochemistry Held in Jerusalem, Israel, 13-16 April 1981. Springer, Dordrecht, the Netherlands.

Bittner, N., Trauer-Kizilelma, U., and Hilker, M. 2017. Early plant defence against insect attack: Involvement of reactive oxygen species in plant responses to insect egg deposition. Planta 245:993-1007.

Brot, N., and Weissbach, H. 2000. Peptide methionine sulfoxide reductase: Biochemistry and physiological role. Pept. Sci. 55:288-296.

Bürger, M., and Chory, J. 2019. Stressed out about hormones: How plants orchestrate immunity. Cell Host Microbe 26:163-172.

Cui, L., Zheng, F., Zhang, D., Li, C., Li, M., Ye, J., Zhang, Y., Wang, T., Ouyang, B., Hong, Z., Ye, Z., and Zhang, J. 2022. Tomato methionine sulfoxide reductase B2 functions in drought tolerance by promoting ROS scavenging and chlorophyll accumulation through interaction with catalase 2 and RBCS3B. Plant Sci. 318:111206.

Darden, T., York, D., and Pedersen, L. 1993. Particle mesh Ewald: An $N\cdot\log(N)$ method for Ewald sums in large systems. J. Chem. Phys. 98:10089-10092.

DeLano, W. L. 2002. The PyMOL Molecular Graphics System. DeLano Scientific, San Carlos, CA.

Dhindsa, R. S., Plumb-Dhindsa, P., and Thorpe, T. A. 1981. Leaf senescence: Correlated with increased levels of membrane permeability and lipid peroxidation, and decreased levels of superoxide dismutase and catalase. J. Exp. Bot. 32:93-101.

Ding, P., Fang, L., Huang, S., Zhu, J., Wang, G., Xia, G., and Chen, F. 2021. Wheat plastidial methionine sulfoxide reductase MSRB3.1 interacts with haem oxygenase 1 to improve osmotic stress tolerance in wheat seedlings. Environ. Exp. Bot. 188:104528.

Dokka, N., Bagri, J., Rathinam, M., Tyagi, S., Prathibha, M. D., Vinutha, T., Prashat, G. R., Sheshshayee, M. S., Dash, P. K., Pareek, A., and Sreevathsa, R. 2024. Decoding nature's defense dance: Mechanistic insights into biochemical and metabolic shifts in *Cajanus cajan* and *Cajanus platycarpus* during combat with the lepidopteran pest *Helicoverpa armigera* provide evidence for non-host plant immunity. Plant Stress 13:100528.

Emmons, C. L., and Peterson, D. M. 2001. Antioxidant activity and phenolic content of oat as affected by cultivar and location. Crop Sci. 41:1676-1681.

Erb, M., and Reymond, P. 2019. Molecular interactions between plants and insect herbivores. Annu. Rev. Plant Biol. 70:527-557.

Felton, G. W., Donato, K. K., Broadway, R. M., and Duffey, S. S. 1992. Impact of oxidized plant phenolics on the nutritional quality of dietar protein to a noctuid herbivore, *Spodoptera exigua*. J. Insect Physiol. 38:277-285.

Foyer, C. H., and Noctor, G. 2005. Redox homeostasis and antioxidant signaling: A metabolic interface between stress perception and physiological responses. Plant Cell 17:1866-1875.

Gershenzon, J., and Ullah, C. 2022. Plants protect themselves from herbivores by optimizing the distribution of chemical defenses. Proc. Natl. Acad. Sci. U.S.A. 119:e2120277119.

Goggin, F. L., and Fischer, H. D. 2022. Reactive oxygen species in plant interactions with aphids. Front. Plant Sci. 12:811105.

Gondor, O. K., Janda, T., Soós, V., Pál, M., Majláth, I., Adak, M. K., Balázs, E., and Szalai, G. 2016. Salicylic acid induction of flavonoid biosynthesis pathways in wheat varies by treatment. Front. Plant Sci. 7:1447.

Gustavsson, N., Härndahl, U., Emanuelsson, A., Roepstorff, P., and Sundby, C. 1999. Methionine sulfoxidation of the chloroplast small heat shock protein and conformational changes in the oligomer. Protein Sci. 8:2506-2512.

Hazra, A., Varshney, V., Verma, P., Kamble, N. U., Ghosh, S., Achary, R. K., Gautam, S., and Majee, M. 2022. Methionine sulfoxide reductase B5 plays a key role in preserving seed vigor and longevity in rice (*Oryza sativa*). New Phytol. 236:1042-1060.

Hess, B., Bekker, H., Berendsen, H. J. C., and Fraaije, J. G. E. M. 1997. LINCS: A linear constraint solver for molecular simulations. J. Comput. Chem. 18:1463-1472.

Hu, D., Guo, Q., Zhang, Y., and Chen, F. 2023. Maize methionine sulfoxide reductase genes *ZmMSRA2* and *ZmMSRA5.1* involved in the tolerance to osmotic or salinity stress in *Arabidopsis* and maize. Plant Mol. Biol. Rep. 41:118-133.

Jacques, S., Ghesquière, B., De Bock, P.-J., Demol, H., Wahni, K., Willems, P., Messens, J., Van Breusegem, F., and Gevaert, K. 2015. Protein methionine sulfoxide dynamics in *Arabidopsis thaliana* under oxidative stress. Mol. Cell. Proteomics 14:1217-1229.

Juszczak, I., and Baier, M. 2014. Quantification of superoxide and hydrogen peroxide in leaves. Pages 217-224 in: Plant Cold Acclimation: Methods and Protocols. D. K. Hincha and E. Zuther, eds. Springer, New York, NY.

Labudda, M., Tokarz, K., Tokarz, B., Muszyńska, E., Gietler, M., Górecka, M., Różańska, E., Rybarczyk-Płońska, A., Fidler, J., Prabucka, B., Dababat, A. A., and Lewandowski, M. 2020. Reactive oxygen species metabolism and photosynthetic performance in leaves of *Hordeum vulgare* plants co-infested with *Heterodera filipjevi* and *Aceria tosichella*. Plant Cell Rep. 39:1719-1741.

Laskowski, R. A., MacArthur, M. W., and Thornton, J. M. 2006. *PROCHECK*: Validation of protein-structure coordinates. In: International Tables for Crystallography, Volume F: Crystallography of Biological Macromolecules. M. G. Rossmann and E. Arnold, eds. Springer, Dordrecht, the Netherlands.

Livak, K. J., and Schmittgen, T. D. 2001. Analysis of relative gene expression data using real-time quantitative PCR and the $2^{-\Delta\Delta C_T}$ method. Methods 25:402-408.

MacKerell, A. D., Jr., Bashford, D., Bellott, M., Dunbrack, R. L., Jr., Evanseck, J. D., Field, M. J., Fischer, S., Gao, J., Guo, H., Ha, S., Joseph-McCarthy, D., Kuchnir, L., Kuczera, K., Lau, F. T. K., Mattos, C., Michnick, S., Ngo, T., Nguyen, D. T., Prodhom, B., Reiher, W. E., III, Roux, B., Schlenkrich, M., Smith, J. C., Stote, R., Straub, J., Watanabe, M., Wiórkiewicz-Kuczera, J., Yin, D., and Karplus, M. 1998. All-atom empirical potential for molecular modeling and dynamics studies of proteins. J. Phys. Chem. B 102:3586-3616.

Martí-Guillén, J. M., Pardo-Hernández, M., Martínez-Lorente, S. E., Almagro, L., and Rivero, R. M. 2022. Redox post-translational modifications and their interplay in plant abiotic stress tolerance. Front. Plant Sci. 13:1027730.

Mellors, A., and Tappel, A. L. 1966. The inhibition of mitochondrial peroxidation by ubiquinone and ubiquinol. J. Biol. Chem. 241:4353-4356.

Mithöfer, A., and Boland, W. 2012. Plant defense against herbivores: Chemical aspects. Annu. Rev. Plant Biol. 63:431-450.

Parrinello, M., and Rahman, A. 1981. Polymorphic transitions in single crystals: A new molecular dynamics method. J. Appl. Phys. 52:7182-7190.

Porebski, S., Bailey, L. G., and Baum, B. R. 1997. Modification of a CTAB DNA extraction protocol for plants containing high polysaccharide and polyphenol components. Plant Mol. Biol. Rep. 15:8-15.

Rathinam, M., Mishra, P., Mahato, A. K., Singh, N. K., Rao, U., and Sreevathsa, R. 2019. Comparative transcriptome analyses provide novel insights into the differential response of Pigeonpea (*Cajanus cajan* L.) and its wild relative (*Cajanus platycarpus* (Benth.) Maesen) to herbivory by *Helicoverpa armigera* (Hübner). Plant Mol. Biol. 101:163-182.

Rathinam, M., Roschitzki, B., Grossmann, J., Mishra, P., Kunz, L., Wolski, W., Panse, C., Tyagi, S., Rao, U., Schlapbach, R., and Sreevathsa, R. 2020. Unraveling the proteomic changes involved in the resistance response of *Cajanus platycarpus* to herbivory by *Helicoverpa armigera*. Appl. Microbiol. Biotechnol. 104:7603-7618.

Rathinam, M., Tyagi, S., Konda, A. K., Rengarajan, D., Prashat, G. R., and Sreevathsa, R. 2022. Relevance of methionine sulfoxide reductase(s) (MSR) as candidate proteins in redox homeostasis-mediated resistance response to *Helicoverpa armigera* (Hübner) in the pigeonpea wild relative *Cajanus platycarpus* (Benth.) Maesen. Int. J. Biol. Macromol. 215:290-302.

Rey, P., and Tarrago, L. 2018. Physiological roles of plant methionine sulfoxide reductases in redox homeostasis and signaling. Antioxidants 7:114.
Šali, A., and Blundell, T. L. 1993. Comparative protein modelling by satisfaction of spatial restraints. J. Mol. Biol. 234:779-815.
Shan, X., Zhang, Y., Peng, W., Wang, Z., and Xie, D. 2009. Molecular mechanism for jasmonate-induction of anthocyanin accumulation in *Arabidopsis*. J. Exp. Bot. 60:3849-3860.
Sharma, M. K., Solanke, A. U., Jani, D., Singh, Y., and Sharma, A. K. 2009. A simple and efficient *Agrobacterium*-mediated procedure for transformation of tomato. J. Biosci. 34:423-433.
Singh, S. 2023. Salicylic acid elicitation improves antioxidant activity of spinach leaves by increasing phenolic content and enzyme levels. Food Chem. Adv. 2:100156.
Singleton, V. L., Orthofer, R., and Lamuela-Raventós, R. M. 1999. Analysis of total phenols and other oxidation substrates and antioxidants by means of Folin-Ciocalteu reagent. Methods Enzymol. 299:152-178.
Sinha, P., Singh, V. K., Suryanarayana, V., Krishnamurthy, L., Saxena, R. K., and Varshney, R. K. 2015. Evaluation and validation of housekeeping genes as reference for gene expression studies in pigeonpea (*Cajanus cajan*) under drought stress conditions. PLoS One 10:e0122847.
Smith, D. B., and Johnson, K. S. 1988. Single-step purification of polypeptides expressed in *Escherichia coli* as fusions with glutathione *S*-transferase. Gene 67:31-40.
Tyagi, S., Rathinam, M., Shashank, P. R., Chaudhary, N., Shasany, A. K., and Sreevathsa, R. 2022a. Deciphering of pod borer [*Helicoverpa armigera* (Hübner)] resistance in *Cajanus platycarpus* (Benth.) offers novel insights on the reprogramming and role of flavonoid biosynthesis pathway. Toxins 14:455.
Tyagi, S., Shah, A., Karthik, K., Rathinam, M., Rai, V., Chaudhary, N., and Sreevathsa, R. 2022b. Reactive oxygen species in plants: An invincible fulcrum for biotic stress mitigation. Appl. Microbiol. Biotechnol. 106:5945-5955.
Ullah, C., Chen, Y.-H., Ortega, M. A., and Tsai, C.-J. 2023. The diversity of salicylic acid biosynthesis and defense signaling in plants: Knowledge gaps and future opportunities. Curr. Opin. Plant Biol. 72: 102349.
Van Der Spoel, D., Lindahl, E., Hess, B., Groenhof, G., Mark, A. E., and Berendsen, H. J. C. 2005. GROMACS: Fast, flexible, and free. J. Comput. Chem. 26:1701-1718.
Vieira Dos Santos, C., Cuiné, S., Rouhier, N., and Rey, P. 2005. The Arabidopsis plastidic methionine sulfoxide reductase B proteins. Sequence and activity characteristics, comparison of the expression with plastidic methionine sulfoxide reductase A, and induction by photooxidative stress. Plant Physiol. 138:909-922.
Waadt, R., Schmidt, L. K., Lohse, M., Hashimoto, K., Bock, R., and Kudla, J. 2008. Multicolor bimolecular fluorescence complementation reveals simultaneous formation of alternative CBL/CIPK complexes *in planta*. Plant J. 56:505-516.
Wasternack, C., and Strnad, M. 2019. Jasmonates are signals in the biosynthesis of secondary metabolites — Pathways, transcription factors and applied aspects — A brief review. New Biotechnol. 48:1-11.
Xiao, L., Jiang, G., Yan, H., Lai, H., Su, X., Jiang, Y., and Duan, X. 2021. Methionine sulfoxide reductase B regulates the activity of ascorbate peroxidase of banana fruit. Antioxidants 10:310.
Yan, Y., Tao, H., He, J., and Huang, S.-Y. 2020. The HDOCK server for integrated protein–protein docking. Nat. Protoc. 15:1829-1852.
Yokoyama, R., de Oliveira, M. V. V., Kleven, B., and Maeda, H. A. 2021. The entry reaction of the plant shikimate pathway is subjected to highly complex metabolite-mediated regulation. Plant Cell 33:671-696.
Zhao, W., Ding, P., Guo, Q., Hu, D., Fu, X., Chen, F., and Xia, G. 2022. Interaction of wheat methionine sulfoxide reductase TaMSRB5.2 with glutathione S-transferase TaGSTF3-A contributes to seedling osmotic stress resistance. Environ. Exp. Bot. 194:104731.